CHALMERS

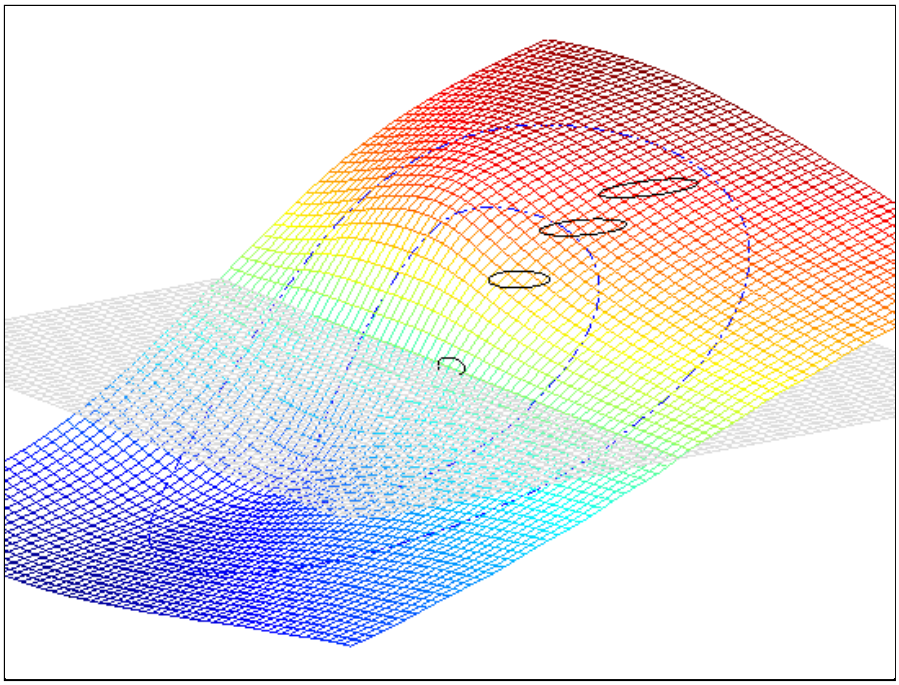

Sensorless Control of a Permanent Magnet Syncronous Machine using Signal Injection

A principal study using Matlab/Simulink and FEM calculations

Master of Science Thesis

RASMUS ANDERSSON
ANDREAS GILLSTRÖM

Department of Energy and Environment
Division of Electric Power Engineering
CHALMERS UNIVERSITY OF TECHNOLOGY
Göteborg, Sweden 2008

Sensorless Control of a Permanent Magnet Syncronous Machine using Signal Injection

A principal study using Matlab/Simulink and FEM calculations

Rasmus Andersson & Andreas Gillström

Sensorless Control of a Permanent Magnet Syncronous Machine using Signal Injection
A principal study using Matlab/Simulink and FEM calculations
RASMUS ANDERSSON
ANDREAS GILLSTRÖM

Department of Energy and Environment
Division of Electric Power Engineering
CHALMERS UNIVERSITY OF TECHNOLOGY

Printed in Sweden by TeknologTryck, Elektroteknologsektionen Chalmers

Abstract

Today the interest for Hybrid electric vehicles (HEV) is high due to their ability to reduce the fuel consumption, which means a reduction in the operation cost as well as in the environmental impact. Weight and volume is important and the machine type with smallest size for a given performance is usually the permanently magnetized synchronous machine (PMSM). To be able to control the PMSM with good performance the position of the rotor has to be known. In terms of space, reliability and cost it would be favorable to replace the mechanical position sensor used today with a so called sensorless control system.

The thesis evaluates the possibilities to use sensorless control for a Permanent Magnet Synchronous Machine (PMSM) used in a hybrid powertrain for heavy vehicles. Different machine configurations are investigated to see if changes can be made facilitating the position detection.

This has been done with simulations in Matlab, Simulink and FEM software. A sensorless method has been implemented in simulations and evaluated on a realistic model of the PMSM in Simulink attained by FEM calculations.

As the problem with sensorless control primarily is related to the signal injection method used at low and zero speed, the focus of the thesis has been at rotation speeds up to 5 electrical Hz. Problems associated with the signal injection method is explained using illustrations describing the machines electromagnetical behavior during loading conditions.

Signal injection methods use the fact that the directions where the permanent magnets are placed in the rotor have the lowest reluctance. It is found that cross saturation effects will change this direction causing an angle error depending on the applied current. This disturbance can however be compensated for to a large extent.

The sensorless control system used in the thesis introduced a limitation in the response time caused by the non ideal filters used to filter the high frequency current response. Optimizations could be done to make the system faster, however it has not been established whether it is possible to make the system equally fast as when using mechanical position sensors.

Evaluation of different machine configurations showed that alterations of the rotor can provide better sensorless performance without deteriorating the machines torque production capabilities.

Keywords: PMSM, Sensorless Control, Signal injection, HEV

Preface

This Master Thesis has been carried out at the Department of Hybrid Technology, Volvo Powertrain AB in Gothenburg from September 2007 to March 2008 under supervision by Mats Alaküla, Senior Scientific Advisor, Volvo Powertrain and Sonja Lundmark, Doctor at the Department of Energy and Environment, Division of Electrical Power Engineering, Chalmers University of Technology. The Thesis is the final part of our degree in Master of Science at Chalmers University of Technology in Gothenburg.

We would like to take the opportunity to show our gratitude to the persons who have supported us in our work and made our life easier during the last twenty weeks.

Our supervisors Mats Alaküla and Sonja Lundmark for supporting us with invaluable advice and for encouraging us at all time.

Avo Reinap, Doctor at Industrial Electrical Engineering and Automation, Lund University, for profitable help with the FEM simulations.

Helena Berg, Anders Kroon, Elisabeth Adolphsson and all the staff in the hybrid team for their warm welcome, providing us with the opportunity to do this work and for all the "fika" and fruit. Special thanks also for the great support and willingness to answer questions given by the entire team, especially Lars-Göran Ullenius and Johan Hellsing.

And last but not least, Staffan and Britt Dromberg for the excellent service by means of transport, food and shelter during our excursion to Lund.

Göteborg, March 2008

Rasmus Andersson Andreas Gillström

Abbreviations

EMF	Electro Motive Force
FEM	Finite Element Method
FFT	Fast Fourier Transform
HEV	Hybrid Electrical Vehicle
Hf	High frequency
ICE	Internal Combustion Engine
IPMSM	Interior Permanent Magnet Synchronous Machine
MAM	Magnetic Anisotropy Method
MMF	Magnetic Motive Force
PM	Permanent Magnet
PMSM	Permanent Magnet Synchronous Machine
PWM	Pulse Width Modulation
RFO	Rotor Flux Orientation
RTDC	Resolver To Digital Converter
SNR	Signal to Noise Ratio
VSI	Voltage Source Inverter
ZCC	Zero Current Clamping

Table of Contents

1 Introduction

1.1 Background

Increased discussions about the global warming have resulted in an increased interest in the area of hybrid electrical vehicles (HEV). A hybrid electric vehicle is equipped with an electrical motor in addition to the internal combustion engine (ICE). This makes it possible to increase the efficiency of the vehicles propulsion. The most suitable machines for this purpose are permanently magnetized synchronous machines (PMSM).

To control the PMSM in an efficient way the position of the machines rotor has to be known at all time. This has traditionally been accomplished by using a mechanical sensor such as a resolver or an encoder. A mechanical sensor will however occupy a significant amount of space. In a HEV this is a large problem as the space in the powertrain is strictly limited.

The mechanical sensor consists of rotating parts which constitutes a risk for failures that will compromise the systems reliability as the position is crucial for the machines functionality. Accurate mechanical sensors like resolvers or encoders are also expensive making it a considerable part of the drive systems cost.

With these limitations in mind it would be favorable to replace the mechanical sensor with a so called sensorless control system, meaning that the need for a mechanical positions sensor is eliminated. Research in this field has been done for several years. By making electrical measurements it is theoretically possible to determine the position of the rotor. For medium and high rotational speeds of the machine the sensorless control is feasible by means of voltage measurement, but at zero and low rotational speed there are still issues to resolve to achieve a system with good sensorless performance, since the induced voltage at zero speed is zero.

1.2 Objectives

The purpose of this thesis is to investigate and evaluate the possibilities of sensorless control of a permanent magnet synchronous machine (PMSM) used in a hybrid powertrain for heavy vehicles. A strategy for the removal of the machines mechanical position sensor and replacing it by a sensorless control system should be proposed.

Different machine configurations should also be investigated to determine if it is possible to change the machines electromagnetically properties to facilitate the detection of the rotor position. These changes should be done without deteriorating the machines torque production capabilities.

1.3 Methods

The thesis starts with a literature study of research carried out in the field of sensorless control of permanent magnet synchronous machines. This to revise what have already been done and to acquire a physical understanding of the problems associated with sensorless control.

Performance of sensorless control systems on different machine configurations is investigated by simulations. The sensorless control system is implemented in the Matlab toolbox Simulink; the graphical user interface makes it possible to accomplish advanced control systems. To get a realistic model of a PMSM to use in the simulations in which it is possible to make changes in the machine configuration, calculations in Finite Element Method (FEM) environment is used. For this the software FEMM is chosen for its great possibility to control from script, making it possible to automate much of the calculation procedure and in an easy way evaluate results from a large number of simulated machine configurations.

2 Control of electrical machines

To understand the concept of a sensorless control system and why it would be favorable compared to a conventional system, there are some things that are necessary to be familiar with: Why the rotor position is required, how it is attained and how its quality affects the performance and reliability of the control of the machine.

2.1 Field oriented control

The development of power electronics resulted in a renaissance in control of electrical machines. Previously most AC-machines had been connected directly to the grid making it difficult to control speed and torque; consequently DC-machines were used in applications with those control demands. With power electronic components, power supplies with controllable voltage and frequency were designed. This made it possible to develop control methods for AC-machines that allowed both speed and torque control.

A method used for speed control in simpler control systems is the volts-hertz method. Speed control is achieved by varying the supply frequency and by controlling the supply voltage approximate proportional to speed, the magnetization in the machine is kept constant. This control strategy can be used without any kind of speed or position feedback and is called open loop control. [1]

To use open loop control with a synchronous machine the speed has to be varied slowly, this to ensure that synchronism is not lost. [2]

The control method used in most high performance PMSM-drives is the field oriented control which allows both torque and speed control with more precision than the volt-hertz method. Field oriented control with rotor flux orientation (RFO) utilizes the fact that the PMSM-machine in many ways is similar to a DC-machine turned inside out. By transforming to a coordinate system rotating with the same speed as the rotor, voltages and currents become dc-quantities. This is called the synchronous reference frame, or sometimes the direct and quadrature, dq-system. The direct axis, often called d, is aligned with the permanent magnet flux linked with the stator windings and the quadrature axis, called q, is placed orthogonal from that. The stator current can then be divided into a d-directed, flux producing part and a q-component that produces torque. In the control system it will then be easy to control the magnetization and torque production in the machine independently, just like in a dc-machine.[3]

The 3-phase quantities are generally expressed in a two-phase stator stationary coordinate system ($\alpha\beta$). The dq-system is then displaced from the $\alpha\beta$-system with the rotor flux angle, θ_r, as seen in Figure 2-1.

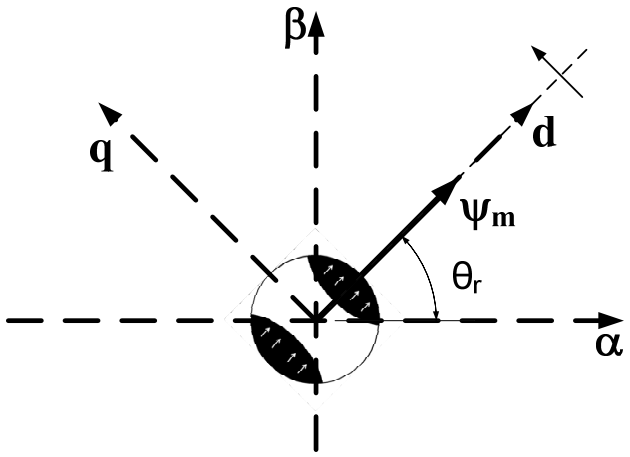

Figure 2-1 Definition of the dq- and αβ- reference frame

To transform quantities between the stationary and the synchronous reference frame the Park-Clark transform is used [1]. In order to be able to carry out the Park-Clark transform, the rotor flux angle has to be known. In conventional PMSM-drives a resolver or encoder can be used for this, but much research has been focused on determining the position without a mechanical sensor. [4], [8]-[18], [20]-[31], [33]-[34]

Regardless how the angle is obtained, accurate knowledge of the rotor position has to be ensured [4] as the d-axis otherwise could become misaligned to the PM flux. This misalignment will result in a deteriorated control of the machine since an incorrect angle can cause a reference applied in the q-direction of the control algorithm to end up in d-direction of the physical machine and vice versa. The machine can then even produce torque in the opposite direction than what was intended, causing the machine to rotate the wrong way.

2.2 Positions sensors

The present rotor position detection in many PMSM machines is carried out with a resolver, which connected to the rotor shaft gives the rotor angle needed in the field oriented vector control. A resolver can be described as a combination of a small electrical motor, built up with a rotor and stator, and a rotating transformer since the voltages are induced between different windings. The stator usually contains three windings while the rotor holds one.

A high frequency reference voltage is applied to one of the stator windings, the primary side of the rotating transformer, exciting a current in the secondary side or the rotor winding. This way, no brushes or slip rings are needed in the resolver. Since this voltage is not used to produce any torque, the amplitude can be kept low, around 5 V, with a frequency at about 5 kHz. The two remaining windings in the stator are placed opposite to the first one, with a mutual distance of 90 degrees. The voltages in the two phase windings will be the injected reference voltage multiplied with sinus and cosines of the angle respectively. This makes the absolute angle, θ_R determinable with $\arctan(u \cdot \sin(\theta_R)/u \cdot \cos(\theta_R))$ and hence, the rotor detection will not be affected by changes in injected voltage that may occur due to temperature changes or ageing. [5] The basic resolver is built as a two pole machine which means that the mechanical and the electrical degrees agree with each other, but with multiple poles, the achieved accuracy can be better. The drawback is that the mechanical and the electrical degree will no longer agree.

Since the resolver is an analogue device, the signal has to be demodulated with a demodulating scheme or a phase locked loop to achieve a digital signal. The comprehensive name for this type of devices is a Resolver to Digital Converter, or a RTDC. [1], [6]

The digital equivalence to a resolver is the encoder. A simple and schematic explanation of the principle behind an encoder can be made by dividing the rotor circumference into small fields, alternatively black and white. With a sensor, e.g. optical or magnetic, it can be determined if the current position is black or white, hence a one or a zero. The absolute position can be determined either by measure the discrepancy from a predefined and detectable zero degrees position, or by use several sensors and construct a binary code that gives the position. The drawbacks with an encoder is that it either needs several sensors that can suffer from disturbances, or has to wait until the zero position mark has passed by, to obtain the absolute position. These facts make the resolver and an RTDC preferable as a rotor position detection device in harsh environments. [7]

2.3 Sensorless control

High quality information about the rotor flux angle is crucial in field oriented control systems. The most common way to attain this information has been to add a dedicated sensor to the rotor shaft. This has a few disadvantages especially in drive systems used in automotive applications. Its physical size is a large drawback when designing the motor. The length of the machine is often critical due to constraints in the powertrain. This makes it sometimes impossible to fit a standard mechanical sensor. [8]

The sensors can also cause problems in terms of reliability as they are sensitive to shock and vibration, optical sensors like encoders are in addition sensitive to dirt. A sensor connected through long cables can also be sensitive to disturbances.[8]

A sensor fulfilling all requirements is often expensive, why removing it would constitute an important cost reduction. A control system that not has to rely on a mechanical position sensor would therefore be favourable, a so called sensorless control system. [9]

Research on this has been done for many years and a lot of methods have been proposed. Many of them have been based on detection of the speed dependent back electromotive force (EMF). This work satisfactory for medium and high speed but fails at low and zero speed. This as the back EMF is reduced with speed and is gradually lost. [10]

To solve this problem, signal-injection methods have been developed taking advantage of that the rotor is salient. By injecting high frequency voltages the difference of inductance in d and q axis direction can be extracted from the resulting high frequency currents. This information will give the position of the rotor. Problems that will arise are low signal to noise ratio (SNR) on the resulting currents making the measurements sensitive to for example noise and non-linearity in the converter. [10]

As the position is determined by the inductance in the rotor there will be problems when the iron becomes saturated as that will decrease the inductance. The problem with saturation is significant in motors for hybrid electric vehicles (HEV) where the torque demand is very high. It is also desirable to achieve a short motor to make it easy to fit. For high torque output, concentrated windings are then needed, increasing the risk for saturation. [9]

3 Existing sensorless rotor position detection methods

There are mainly two different methods to obtain the rotor position without the use of mechanical sensors, the back electromotive force or back EMF method and the signal injection method [11]. In the following chapter, these methods are introduced in terms of operation areas and limitations. A new, third method that uses the characteristics of the magnetic material is also briefly explained. In the last part of the chapter, a description of how the two main methods can be combined is done.

3.1 Back EMF

For medium and high speed, the dominating methods to detect the rotor position without using a mechanical sensor is to make use of the back electromotive force, back EMF, from the motor model. [12]

The underlying theory behind these methods is the motor equation of the stator, in (3.1), expressed in the dq reference frame. In (3.2), the back EMF term, $\mathbf{e}_f$ is defined.

$$\vec{v}_{dq} = L_{dq} \cdot \frac{d\vec{i}_{dq}}{dt} + R_{dq} \cdot \vec{i}_{dq} + \vec{e}_f \qquad (3.1)$$

$$\vec{e}_f = j \cdot \omega_r \cdot \vec{\psi}_{m_{dq}} \qquad (3.2)$$

In (3.1) and (3.2), the inductance, L_{dq}, the resistance, R_{dq}, and the magnetic flux generated from the permanent magnet in the rotor, ψ_{mdq}, are all approximately known quantities. The current, i_{dq} and voltage, v_{dq}, can be measured; hence the motor equation can be solved for the electrical rotor speed, ω_r. Finally an integration of the speed dependant back EMF term, results in an achieved rotor position. [1]

The limitations of the back EMF methods are the fact that the detection possibility is proportional to the speed; the ability diminishes at low rotor speed and stand still. The explanation to this is that the amplitude of the back EMF will be small since $\mathbf{e}_f$, as can be seen in (3.2), is proportional to ω_r. Hence the terms with the inductance and resistance in (3.1) will become dominant compared to the back EMF, meaning that the motor equation element containing the information regarding the position gets to small to detect. [12]

In order to settle the speed at which $\mathbf{e}_f$ no longer is useful, methods determining when the back EMF method becomes unstable has been developed. These methods can be implemented in the control of the machine. [13]

The methods based on the motor model usually detect the back electromotive force vector and extracts information about rotor position with either an open or a closed-loop observer [4]. A rule of thumb for the observers is that they have to be faster than the system they observe, but slow enough to suppress noise and other type of disturbances [8].

Open loop observers suffers from sensitivity to system noise and changes in the stator resistance. During operation the stator resistance can increase with up to 50% due to heat. The problem with changing resistance becomes evident at low speed as the voltage drop over the stator resistance then is of the same magnitude as the back EMF. [4]

As back EMF based rotor position detection methods already works satisfactory for automotive applications during medium and high speed, e.g. utilized in a test vehicle from Daimler Chrysler [8], this paper will not look any further into this subject.

3.2 Signal injection

The basic idea behind the signal injection methods is to add a high frequency signal in order to obtain the rotor position. The high frequency, typically 0.5 to 3 kHz [14], means that the resistance in the motor can be neglected and the current will depend on the inductance only [15], [16]. The applied signal can either be added with superposition on top of the fundamental voltage, or by modifying the fundamental PWM pattern to contain a voltage pulse that can be used to track the rotor position [17]. The following subchapter shortly explains the physics behind the phenomena and the two different ways to inject the high frequency signal. Finally some resent research on improvements is mentioned.

3.2.1 Theory behind signal injection

The saliency, on which the signal injection techniques are based on, originates from either an asymmetrical rotor design or from the saturation caused by the permanent magnets. [11], [18]

In an internal permanent magnet synchronous machine, IPMSM, the permanent magnets are buried in the rotor core. The consequence is a spatial saliency since the d-directed flux will pass trough magnet material instead of iron for some part. The flux paths are shown in Figure 3-1.

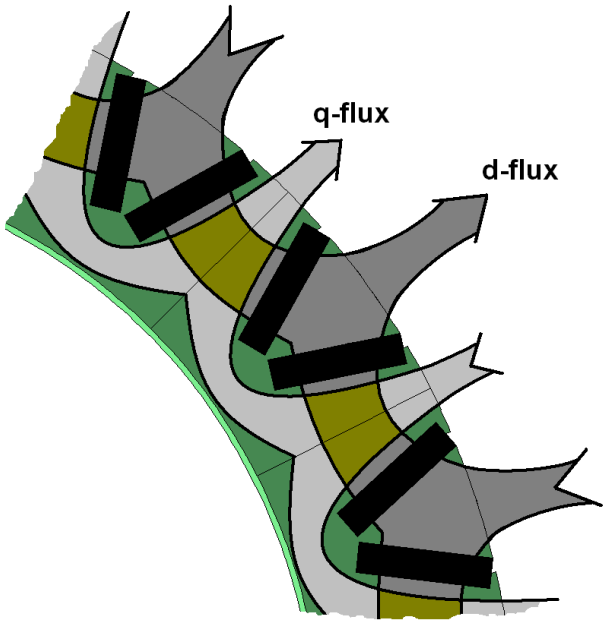

Figure 3-1 Flux paths in a V-shaped IPMSM

As the relative permeability of a magnet is close to one, which is comparable to air from a flux point of view, the d-directed stator flux will appear to face a larger air gap compared to the flux in the q-direction. In (3.3) it is stated that the reluctance, $\Re$, is inversely proportional to the permeability, μ, and with the relative permeability of iron being at least 10^3 times higher than air [19], the flux will experience more resistance in the d-direction passing trough iron for a shorter distance.

$$\Re = \frac{\ell}{\mu \cdot A} \tag{3.3}$$

$$\psi = \frac{mmf}{\Re} \tag{3.4}$$

$$\psi = L \cdot i \tag{3.5}$$

According to (3.4), the flux linkage, ψ can be higher for a smaller reluctance and a constant mmf, or magnetic motive force; hence the flux will flow more easily in the q-direction. These facts in combination with (3.5), the relation between inductance, L, and flux linkage, suggests that larger air gap leads to lower permeability, meaning a larger reluctance that gives lower flux and eventually lower inductance. Hence, for an IPMSM such as the one shown in Figure 3-1 above, the inductance in d-direction, L_d, will be lower than the q-directed, L_q, something that can be and are used to detect the rotor position.

If the permanent magnets instead are mounted on the surface of a cylindrical rotor core, there will be no difference between the d- and q-directed air gaps that can be used for rotor position detection. In this case the saliency instead originates from magnetic saturation in the iron. Since the d-direction is magnetized with PM as well, the stator flux linkage as a function of stator current in the d-direction is offset by the PM flux. The increased amount of flux in d-direction means a reduction in the relative permeability, μ_r and hence according to (3.3) to (3.5) lower inductance. The consequence is that the d-directed stator flux gets slightly lower than the q-directed and the rotor appears to be salient. However, the saliency caused by this phenomenon is much smaller then that caused by spatial differences, hence, the signal injection method is seldom used on surface mounted PM machines [20].

The problem with the saliency based signal injection methods appears when the electrical load is increased. With a large torque demand, the current to the machine has to be higher, which means that the magnetic flux in the iron parts will increase as well. Eventually the iron reaches magnetic saturation and the flux linkage will no longer be able to increase. This is illustrated in the B-H curve for a type of laminated steel in Figure 3-2, where it can be seen that the flux density in the iron increases steeply up to a certain level, after which any further increase would require a vast increase in the current density.

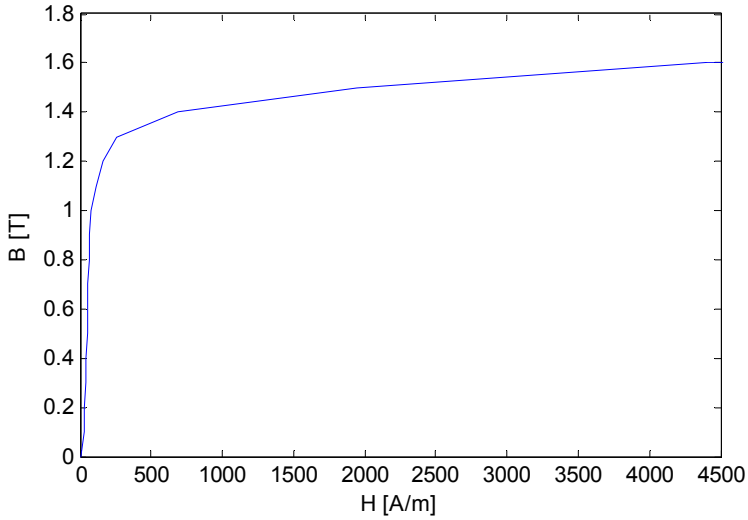

Figure 3-2 B-H curve for magnetic steel

According to (3.5), the inductance is forced to decrease if the current continue to increase after the saturation state is reached.

Due to that the saturation of the iron is a nonlinear phenomenon, the inductances will decrease nonlinearly and the foundation of which the signal injection method is based on is interrupted.

Further on, the d-directed inductance will not be as much influenced as the q-directed, L_q which complicates the saturation dependent position determination methods even further [13], [21].

Another source of disturbance is the cross-saturation; an applied current in d- or q-direction affects both the d- and q- inductances. This phenomenon can be explained by imagining that the iron contains a limited number of flux carriers that transports the magnetic flux, that is, if some of the available flux carriers have to be used to transport flux in one direction, the ability to transport flux in the other direction will decrease. Hence the inductance will change even if the current is applied in the other direction. In Figure 3-1 it can be seen that the different flux paths cross each other. If the iron along one of the flux paths is saturated, the other flux path will also be affected due to the saturation in the crossing.

3.2.2 Superposition injection scheme

In the superposition method, the high frequency voltage signal is created by the converter and superimposed on top of the fundamental voltage. This means an upper limit on the frequency of the injected signal; it has to be low enough to be realized by the converter [22]. The result is a measurable, high frequency current response containing information about the rotor position.

The technique can be divided into several different methods with different approaches to obtain the rotor position. The injected high frequency signal can be rotating or pulsating, injected in stationary, $\alpha\beta$-, or rotating, dq-reference frame and be injected as currents added to the references in to the regulator or as voltages added directly before the motor. The common part for all methods is that the information is obtained by evaluating the current response given by the motor due to the saliency, by adding a high frequency signal on top of the fundamental signal. [11]

If the high frequency signal is superimposed in a dq-reference frame, the rotor angle information is attained by using the fact that the d- and q-axis are decoupled. This means that if the high frequency signal is added in an estimated d-direction there should be no high frequency current response in the q-direction, which can be used to regulate the estimated d-direction to equal the real one. This is done by demodulation of the signal into a DC current, proportional to the rotor position estimation error and sent to an observer that updates the estimated speed and angle until the error reaches zero, that is, until the estimated rotor angle equals the real one. The observer is modeled on a mechanical model of the motor, containing estimations of the inertia and torque and if these estimations can be made correctly, the speed and rotor position can be followed with almost no lagging. [12]

The advantage of this type of superimposed signal injection methods is that the torque ripple will be minimized as there, when the angle estimation is correct, will be no high frequency current on the torque producing q-current. On the other hand, problems will occur when the fundamental currents are applied since this causes cross saturation which counteracts with the idea of decoupled axis and thereby makes the method less accurate.

When the high frequency signal is injected in the stationary, $\alpha\beta$-reference frame the differences in the inductance is the main source of information. The signal is injected as voltages with constant amplitude, rotating in the $\alpha\beta$-reference frame, leading to constant amplitude in the induced flux. According to (3.5) the varying inductance in combination with the constant flux will make the high frequency current response dependent on if the flux is directed along the d- or q-axis. Since L_d is smaller than L_q, the amplitude of the current will be higher when directed along the d-axis, something that can be used to obtain the rotor angle. [11]

3.2.3 PWM pattern modification

The other type of signal injection is the voltage pulse test method. Like in the superposition method the only motor parameter in the high frequency model of the motor voltage equation that varies is the inductance. This means that if the derivative of the current caused by the applied voltage is measured, the inductance can be calculated. In the voltage test pulse method the PWM switching pattern is modified. At the beginning of the PWM pattern a test voltage vector is applied and after about 5 μs the current derivative is measured in all three phases. Last in the PWM pattern a test voltage vector with the opposite sign is applied and the current derivative in all three phases is measured again. With this information the inductances can be calculated. By using voltage vectors with opposite sign the effects of voltage drop in resistances and the back EMF are canceled, even though these effects can be neglected in the high frequency model. [10]

3.2.4 Recent research

Due to the many difficulties concerning signal injection methods much research has been done to refine the methods. When studying scientific articles from the last few years it appears that most studies has been concentrated on finding a general sensorless method that can be directly applied to most commercial PMSMs. Some years back there where more attempts to make the detection easier by making changes in the rotor configuration. One example is [23] from 1998, where attempts to improve position estimation by placing a sensing winding in the rotor was made. The winding was placed to link with the d-axis flux only and not with the q-axis flux. Since high frequency voltages injected in the stator induces currents in the winding, the stator inductance becomes reduced when the stator is aligned with the d-axis but not when aligned to the q-axis. This increased difference of inductance in d- and q-direction was supposed to increase the accuracy of position determination. A drawback

with such a sensing coil is the decrease of torque that in the paper was said to be approximately proportional to the reduction of iron material to fit the rotor winding.

In [22] the motor equation is expressed in stationary, αβ-reference frame, but rewritten to contain the inductances expressed as L_d and L_q from the rotating dq-reference frame, making them dependent on the angle. This results in a so called Extended back EMF term, which not is speed dependent. The prerequisites for this method are that there has to be a difference in the d- and q-directed inductance, which is fulfilled with a salient rotor, and that the derivative of the d-current must not be equal to zero. This is realized with an applied high frequency signal to the reference current. The advantage with this method compared to other is pointed out to be the ability to detect the polarity of the d-axis directly, which other methods has had problems to do. The disadvantage is that the method is volatile and easily becomes unstable.

A solution to the fact that the values of L_d and particularly L_q will change during saturation has been presented in [9]. By modeling the motor using FEM calculations, a non linear voltage equation is achieved and hence better estimations can be made. Another approach to the same problem is presented in [18], where the inductances are expressed as Fourier series that depends on rotor position and stator voltages. However, in both methods, the problem of acquiring exact measurement data remains.

As the injected signal amplitude is small compared to the fundamental voltage and current, distortions can easily deteriorate the information. One way to increase the SNR is to increase the signal, e.g. the amplitude of the injected voltage, something that means increased losses and torque ripple. This makes it more favorable to try to decrease the noise, originating from for example errors in the measurement equipment, something that has been suggested in [24].

Another source of distortions is nonlinearities in the inverter, especially if the machine is supplied by a standard PWM Voltage source inverter (VSI). According to [25] the Zero Current Clamping, or ZCC, is the largest cause of distortions in the carrier signal. In that paper it is shown that the ZCC effect is related to the inverter dead time and occurs when a phase current crosses zero and the current path changes from one transistor to a diode. Moreover, in [26] it is stated that as the transistors not are turned on and off instantaneously, ZCC is caused by two things. First the extinction of the current in the freewheeling diode which disconnects the phase leg from the bus for a period of the dead time and also the larger commutation time at low current levels due to parasitic capacitance in the diode.

Reference [27] has stated that if the applied high frequency voltage vectors are not synchronized with the rotor rotation there will be induced eddy currents that will add losses to the iron. The proposed solution is to add the eddy current effects to the high frequency model to improve the accuracy of the estimated angle.

3.3 Magnetic anisotropy method

A new method to determine position during low-speed and in stand-still is the Magnetic Anisotropy Method (MAM). Instead of using saliency in the rotor to determine the position, anisotropies effects in the permanent magnets are used. The physical properties are different in different directions depending on the direction of the measurement. The frequency of the applied carrier voltage is set to 100-500 kHz instead of 0.5-3 kHz that is more common in other signal injection methods; hence an additional signal generator has to be utilized. In industrial applications this has to be a chip, with the ability to generate such a high signal. High frequency voltages are applied in one phase and the response is measured in all 3 phases. This type of measurement is performed for all three phases and from this information the rotor position can be extracted.

Unfortunately this method is undeveloped, e.g. the temperature dependence of the anisotropic properties has not been examined and satisfactory results have not been obtained in practical experiments. This means that the research in the area is concentrated in trying to explain the phenomena physically.

The great advantage with this method would be that it has the theoretical possibility to work for salient as well as non salient motors, where the permanent magnets do not saturate the stator teeth. [14]

3.4 Possibility to combine different methods

As a conclusion, the signal injection method has the big advantage of its capability to detect the rotor position at low and zero speed [15]. On the other hand the drawbacks are that it requires high accuracy measurement equipment with good capability to handle noise and disturbances and precise signal processing [15]. It is not suitable as a replacement for back EMF methods at higher speeds as additional losses will be added due to the extra signal [28]. The high frequency signal added to the fundamental voltage requires some modulation space and will also decrease the maximum available voltage vector. In applications with high torque demand saturation effects still remains a serious concern. Furthermore, the reliability and noise specification required in an automotive application is not yet fulfilled [8].

On the other hand, the large amount of research on the back EMF method has made it a reliable sensorless rotor angle detection method for medium and high speeds that, as mentioned above, already has been implemented in the automotive industry. Combining the abilities of the two methods makes it possible to create a sensorless current control that could handle the entire speed range [28], [29]. At low speeds signal injection can be used and as soon as the back EMF method reaches stability, it succeeds. The changeover can be realised with a step that is activated once the EMF-method is stable, but in order to acquire a more smooth conversion an arctan function can be used [30].

Considering that the part of the sensorless control system not yet fully developed is position detection at standstill and low speeds, the focus in this paper has been put on understanding the problems and trying to suggest improvements that can facilitate the rotor detection at these conditions.

4 Simulation environment

In the work of investigating the possibilities of sensorless operation of the PMSM machine a good simulation environment had to be constructed. The ambition was to make as much as possible of the calculations automated to allow easy changes in the machine configuration and quickly evaluate its effect on the sensorless performance.

4.1 Matlab/Simulink

To evaluate the sensorless control system on an electrical model of the PMSM machine the Matlab toolbox Simulink appeared to be a good choice. In Simulink advanced control systems can be implemented without too much difficulty thanks to the graphical user interface.

4.1.1 Existing Simulink model

An existing Simulink model of a PMSM machine with control system was attained from the start. The system was developed at Lund University in Sweden where it is used in education. To be as authentic as possible the control system is implemented on a digital form as in a real control system where the inputs are sampled values of the measured signals. The control system is basically a current controller implemented in the dq-reference frame. Based on the reference current and actual current the system calculates new voltage references which is transformed to 3-phase quantities, something that requires a correct angle estimation. The 3-phase reference voltages from the control system are discrete and changes once every switching period. By comparing the 3-phase references with a triangular wave the duty cycles to the IGBTs in the Pulse Width Modulated converter are calculated. As the supply to the PMSM machine is PWM-voltages some of the non-ideal effects found in reality are represented in the simulations.

The model of the PMSM was based on the stator equations in a rotor reference frame described in (4.1) to (4.4).

$$v_d = R \cdot i_d + \frac{d\psi_d}{dt} - \omega_r \cdot \psi_q \tag{4.1}$$

$$v_q = R \cdot i_q + \frac{d\psi_q}{dt} - \omega_r \cdot \psi_d \tag{4.2}$$

$$\psi_d = L_d \cdot i_d + \psi_{pm} \tag{4.3}$$

$$\psi_q = L_q \cdot i_q \tag{4.4}$$

The machine is supplied with a voltage and will consume a certain current. Equation (4.1) to (4.2) can be rewritten to (4.5) and (4.6) which mean that flux in the machine will be the integration of the voltages in the right hand side of the equations. Currents and fluxes in the right hand side of (4.5) and (4.6) will be feedbacks from the previously calculated values. Which current a certain flux will correspond to will then be determined by the inductance as seen in (4.7) and (4.8).

$$\psi_d = \frac{1}{s} \cdot \left(v_d - R \cdot i_d + \omega_r \cdot \psi_q \right) \tag{4.5}$$

$$\psi_q = \frac{1}{s} \cdot \left(v_q - R \cdot i_q + \omega_r \cdot \psi_d \right) \tag{4.6}$$

$$i_d = \frac{\psi_d - \psi_{pm}}{L_d} \tag{4.7}$$

$$i_q = \frac{\psi_q}{L_q} \tag{4.8}$$

In the supplied linear model of the PMSM the inductances were constant values and the flux in d direction was only dependent on the current in d direction and not dependent of the current in the q direction, and vice versa. This is a valid approximation for low current levels. However when the current loading increases the inductance will change due to the saturation effects in the iron. There will also be a cross saturation effect; a change in the d axis flux will cause a change in the q axis current and vice versa. This much more complicated behavior is very important to represent if to simulate the behavior of sensorless control algorithms as the problem with getting these to work much depend on the nonlinear effects.

4.1.2 Nonlinear model

To create a more realistic model of the machine the changes of the inductance due to electric loading has to be characterized. This can be done either by measurements on a machine or by FEM-calculations. As part of the task was to study changes in the rotor configuration FEM calculations is the obvious choice. By performing FEM-calculations for stepwise current loadings in d and q axis and evaluating the resulting flux linkage in the stator coils a relation can be established. This will illustrate saturation as well as cross saturation effects.

4.2 Matlab/FEMM

To accomplish a good model of the PMSM machine many FEM-calculations has to be performed. The flux linkage in the stator coils must be calculated for a large number of current loadings and for several rotor positions. If the simulation environment should be kept dynamic and allow for easy changes in the rotor configuration this has to be an automated process. Therefore it was decided to use the software FEMM which incorporates the use of Lua-script which can be utilized to automate calculation tasks. FEMM is a free calculation software for magnetics, electrostatics, heat flow and current flow. The software only supports 2D calculations, this is however satisfactory as the machine does not change much along the rotor axis, hence effects of the stator end windings can be neglected [31].

4.2.1 Calculations using Lua-script

Lua-script support adds the opportunity to control the complete software from a script file. Geometries can be drawn, materials defined, calculations performed and results presented. That the software is able to be controlled completely from a script file provides the possibility to make use of the powerful FEM-calculation from another program, for example Matlab. By creating a Lua-script file from Matlab, execute it and read the results, it is possible to perform FEM calculations from within Matlab.

4.2.2 Code for design of Radial Flux machines

At Lund University in Sweden (LTH), code for radial flux machine design by FEM-calculations has been developed by Dr Avo Reinap [32]. In the code most parameters for a PMSM can be specified, geometrical measurements, materials, electric loading, type and number of windings, magnet type and much more. A Lua-script with this information is created from Matlab and executed with FEMM that performs the calculations and saves the results to a file which can be read by Matlab. Changes in the configuration can then be

evaluated in terms of torque capability, air gap flux density and other interesting quantities. The different steps are illustrated in Figure 4-1.

Figure 4-1 Flowchart of the data between the different software's

This is a very fast process, a configuration can be finished within a few seconds depending on its complexity, how fine grid that is used for the FEM calculations and the performance of computer used.

To fulfill the requested requirements some changes had to be done to the code. For example the ability to control the distance between the magnet pairs were added, e.g. twice the distance D in Figure 4-2. This as the distance between the magnets forms the path for the q axis flux and could be important for the characteristics of the machine.

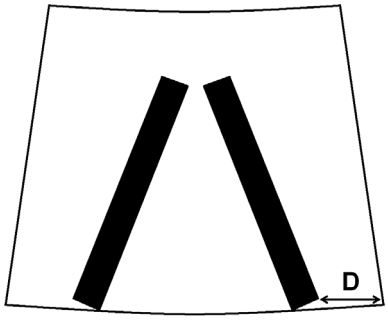

Figure 4-2 Sketch of the rotor configuration

4.2.3 Modeling the PMSM

When modeling the PMSM machine many assumptions were made. The configuration of the rotor and stator is very complex and to achieve an optimal design very much time and effort has to be put in. The idea was instead to accomplish a principal design of a PMSM machine that could be used in a HEV. Approximate outer dimensions of a 120 kW PMSM machine was therefore used. Machines used in HEV are typically short but has a large diameter, this due to constraints in the powertrain length. The short length of the machine will lower the reliability of the FEM-calculations as the end windings effect gets more significant. This should however not constitute in any large problems as the calculations are made essentially to get a principal understanding of how physical changes in the machine affects its electromagnetic dynamics.

The stator of the machine was approximated with a simple geometry with 3 phases and one slot for each pole and phase. For simplicity the windings in the stator was made with only one turn, this means that the results had to be rescaled with the number of turns later according to the specific voltage level and speed the machine should be designed for.

Materials chosen were 0.35 mm laminated iron for the rotor and stator core, plastic bonded NdFeB for the permanent magnets and copper for the electrical windings.

The permanent magnets in the rotor can be placed in many ways as seen in Figure 4-3. The first configuration is surface mounted magnets, the second inset magnets and the third configuration is V-shaped inset magnets.

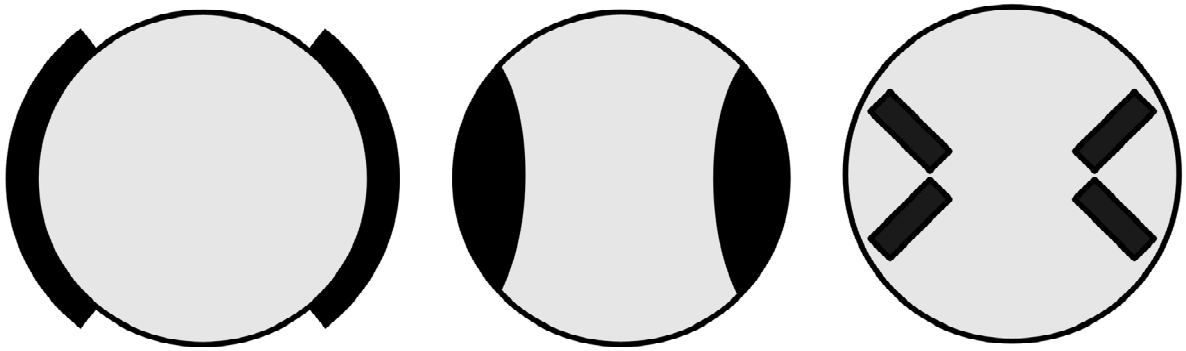

Figure 4-3 Different placement of the permanent magnets in two pole rotor

The V-shaped magnets were chosen for the principal design, which is what is used in the motor configuration presented by Toshiba for a hybrid truck [33]. Toshiba has also added cavities with low reluctance material at some specific points, this to be able to control the flux path more precise. This was omitted in the principal design due to the great complexity this would add to the modeling as well to the simulations. Also the mechanical strength of the rotor was not considered. When placing the magnets very close to the air gap to avoid leakage flux it can be seen in Figure 4-4 that the iron in between the V shaped magnets will just barely be attached to the iron in the rest of the rotor, resulting in poor mechanical strength.

A picture of the smallest possible symmetry piece of the principle design can be seen in Figure 4-4. It is also on this symmetry piece of the rotor and stator the calculations are made, results from the entire machine can then be attained by making use of the symmetry.

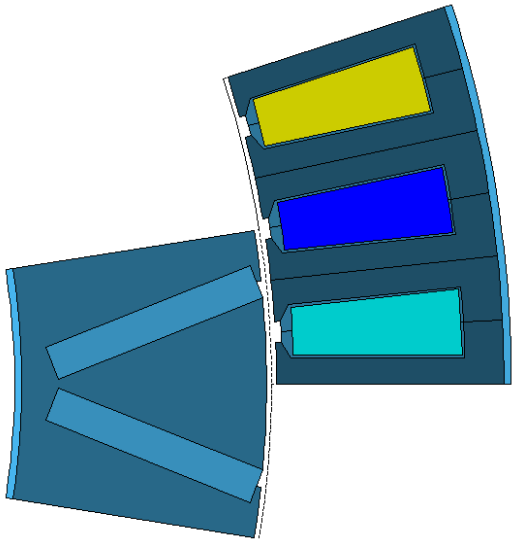

Figure 4-4 A fragment of a symmetrical motor configuration

4.3 Merging FEMM, Matlab and Simulink

To get a desirable dynamic simulation environment, work procedures for using the different software together had to be prepared. A good way to exchange the data between the software also had to be established.

4.3.1 Calculation of flux linkage and torque

A reasonable geometry is created in the code for a radial flux machine design with the prerequisites determined in chapter 4.2.3. To understand the behavior of the saturation and cross saturation effects calculations has to be performed for several currents in the d and q direction. In a Lua-script the defined configuration is imported and the script is set up to perform calculations for a large number of current loadings in the d and q axis direction, as well as all combinations of them. The calculations are also performed for several rotor positions as the torque and flux linkage changes with the position due to interaction between the permanent magnets in the rotor and the stator poles. In the simple geometry used with one slot for each pole and phase these changes are repeated periodically with 60 electrical degrees. To get a more realistic model of the PMSM it would be possible to characterize this angle dependent variation. This would however generate large amount of data and increase the simulation time and complexity. Therefore, it was decided to make the calculations for a number of rotor positions within these 60 electrical degrees and compute an average. If the number of slots per pole and phase are increased, these variations get lower amplitude and higher frequency, which can be favorable in that respect that it gives a smoother torque. This would however greatly increase the simulation time as the lowest symmetry part is increased to several poles of the machine, why this has been omitted.

When FEMM has finished all calculations specified in the Lua-script the result file can be read by Matlab, the steps can be seen in Figure 4-5.

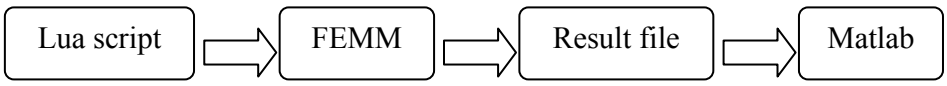

Figure 4-5 Flowchart of the data between the used software's

The result file is a text file containing one row for each calculation on which the rotor angle, electrical loading and calculated torque and flux linkage is printed. Flux linkages are transformed to the rotor reference frame and mean values for the different rotor angles are computed. The attained values are from the least possible symmetry piece of the machine; to get the correct values for the complete machine the flux linkage and torque has to be multiplied by the number of symmetry pieces that the machine consists of. As the number of turns in the stator windings are set to one during calculations, the flux linkage and current has to be scaled according to the real number of turns. How many turns there are in a real machine depends on which voltage level and nominal speed it is designed for.

The machine is assumed to be supplied from a 600 V DC-source by a three phase inverter as in Figure 4-6.

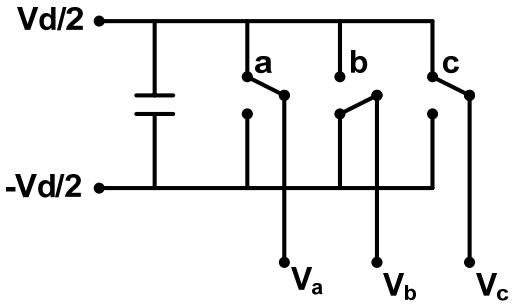

Figure 4-6 Three phase inverter

When using a PWM inverter with space vector modulation there are 6 available space vectors from the inverter. They are created by having the three IGBTs turned on or off in different combinations. The vectors V_1-V_6 can be seen in Figure 4-7, together with the zero vector, V_0 that has the length 0. By switching very fast between these vectors a mean voltage vector can be achieved anywhere inside the hexagon. The vectors V_1-V_6 all have the length $V_{dc} \cdot \sqrt{2/3}$ in the power invariant αβ-system. However, the largest vector that can be put out at all time is the vector V_{base}. Simple geometry shows that the length of vector V_{base} is $V_{1-6} \cdot \sqrt{3}/2$. This means that the largest vector that can be put out at all time is $V_{dc}/\sqrt{2}$.

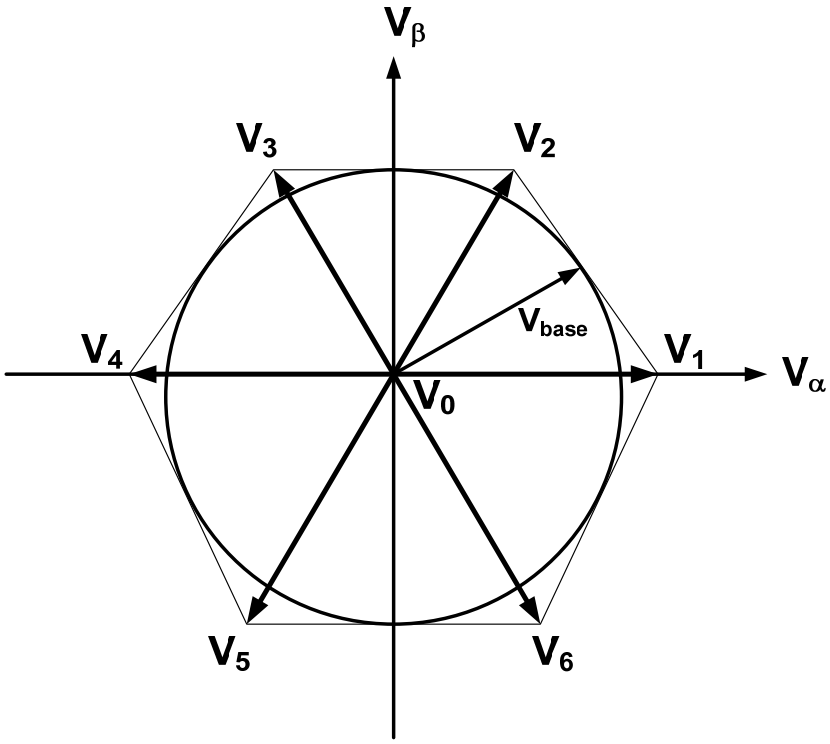

Figure 4-7 Space vector diagram

In steady state, the stator voltage the in rotor reference frame can be described as in (4.9). At higher speed the resistive voltage drop in the stator windings can be neglected and the voltage depends on the term in the right hand side of (4.10) which is the back EMF.

$$\overrightarrow{u_s} = R \cdot \vec{i_s} + j \cdot \omega_{el} \cdot \vec{\psi} \tag{4.9}$$

$$\overrightarrow{u_s} \approx j \cdot \omega \cdot \vec{\psi} \tag{4.10}$$

To be able to control the machine, the back EMF should not exceed the maximum available voltage vector. As seen in (4.11) to (4.13) this gives a condition for the maximum flux vector that could be created at different speeds. In (4.13) there is a control margin of 10% added to insure that the vector could be created.

$$\left|\overrightarrow{u_s}\right| \le \frac{V_{dc}}{\sqrt{2}} \tag{4.11}$$

$$\omega_{el} \cdot \left|\overrightarrow{\psi_s}\right| \le \frac{V_{dc}}{\sqrt{2}} \tag{4.12}$$

$$\left|\overrightarrow{\psi_s}\right| \le \frac{V_{dc}}{\omega_{el} \cdot \sqrt{2} \cdot 1.1} \tag{4.13}$$

At nominal speed and zero torque the flux in the machine is created by the permanent magnets and the nominal stator current together. The number of turns in the stator windings has then been established by the highest integer of turns that doesn't make the induced back EMF at nominal speed exceed the maximum voltage vector. When performing the rescaling, calculated flux linkages are multiplied and the currents divided with the number of turns.

Having the correct values for the complete machine, surface plots of the flux linkage in the d and q axis direction can be made as a function of current in the d and q axis direction. As the flux linkage and current is known, the inductance can be calculated and also plotted in surface plots. Together with the surface plot of the torque these three dimensional figures gives a good understanding of how the machines electromagnetic dynamic changes when the electrical loading increase.

4.3.2 Integration of flux linkage tables in Simulink

To use the results from the FEM-calculations in a nonlinear model of the PMSM machine in Simulink the data should be presented as current as a function of flux linkage, the opposite from what's received from FEMM calculations. Transforming these results is complicated by the fact that all values are interconnected due to the cross saturation. The Matlab code performing the transformation can be seen in Appendix A. The data is saved to a file and imported into Simulink where it is implemented in two multidimensional look-up tables. The path of the data can be seen in Figure 4-8.

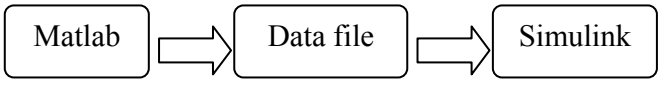

Figure 4-8 Flowchart of data used in the look-up tables

4.3.3 How to evaluate different geometries

In the configuration of the PMSM there are numerous parameters to change and study the effects of. To be able to compare the different geometries they should have about the same

torque production capabilities. This has been approximately accomplished by comparing configurations with similar permanent magnet flux linked to the stator, as this means similar magnetically produced torque, though disregarding the reluctance torque. The different rotor configurations, however will mean different reluctance torque, hence the total amount of torque might still vary, something that has to be considered in an eventual evaluation. A very large number of geometries were first created for which flux in d axis direction was calculated with unloaded windings, e.g. the flux from the permanent magnets. The results were plotted in Matlab which made it easy to isolate the geometries with the same permanent magnet flux, these were selected and more extensive calculations performed.

5 Implemented sensorless rotor position detection

In order to perform simulations with a sensorless control system, a working model had to be implemented in Simulink. In the following chapter a short presentation of a widely used method are carried out. This is followed up by a method developed from the knowledge and physical understanding obtained from studying the literature.

5.1 Existing method

After reading a vast amount of scientific papers, it was decided to look a bit further into [12] since a lot of the more recent articles containing improvements had built their sensorless control from this paper, making it a reliable and relatively well tested technique.

This method uses the similarities between a PMSM and a resolver. The fact that the d- and q-axis flux linkages are decoupled is utilized by applying the high frequency signal to give a flux linkage in the estimated q-axis direction only. A controller similar to a resolver to digital converter (RTDC) can then be used to adjust the estimated rotor angle to follow the actual one by regulating the direct axis current response to zero. This occurs when the applied flux is directed in the actual q direction, hence when the estimated position equals the real one. However, the cross saturation associated with high fundamental currents causes a problem to the method since an applied flux in the q-direction affects the d-axis as well. The consequence is a deviation in the angle estimation when torque producing currents are applied. To avoid the offset, the angle has to be measured and compared to the actual angle in advance and compensated for.

5.2 Developed method

In order to keep the physical understanding of the sensorless technique, it was decided to develop a fundamental method using the knowledge obtained from studying existing sensorless rotor position detection methods. Below, the theory behind the method and the realization in Simulink are explained.

5.2.1 Theoretical explanation

As described, the physical phenomena in an IPMSM can be used to detect the rotor position by adding a high frequency voltage to the motors supply voltage. In the method used in this paper, a rotating high frequency voltage, $v_{si}^{\alpha\beta}$ described in (5.1), is superimposed in the αβ-reference frame at the output of the current controller.

$$\begin{aligned} v_{si}^{\alpha} &= V_{si}\cos(2\pi \cdot f_{si} \cdot t) \\ v_{si}^{\beta} &= V_{si}\sin(2\pi \cdot f_{si} \cdot t) \end{aligned} \tag{5.1}$$

The low amplitude, V_{si} and high frequency, f_{si} makes the inertia in the machine sufficient to prevent the rotor from being affected by the extra, alternating torque produced by the injected voltage.

The added high frequency α- and β-voltages are applied with a 90 degrees phase shift, constituting of a rotating voltage that causes a rotating magnetic flux through the rotor. Since the amplitude of the voltage is constant, the amplitude of the flux, ψ will be constant as well, making it a circle, described in Figure 5-1.

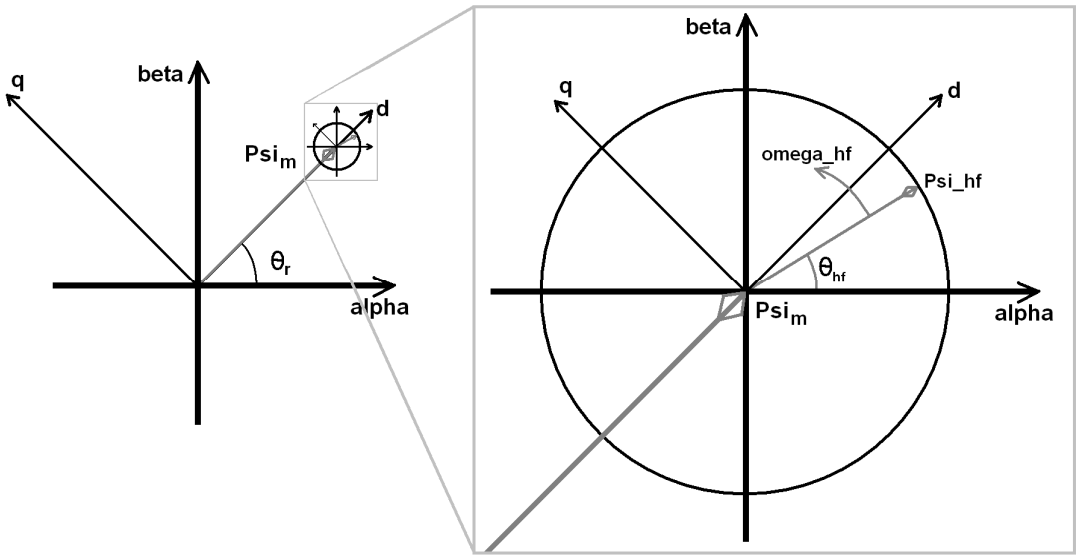

Figure 5-1 Rotating stator flux linkage with constant amplitude

As the reluctance along the direct axis is larger than along the q axis, the amplitude of the resulting current vector, i_{hf}, in to the motor will be higher when directed towards the d axis compared to when directed to the q axis hence dependent on the high frequency angle, θ_{hf}. The varying amplitude of the current can be described as the ellipse in Figure 5-2, where the higher reluctance in the direct direction results in higher amplitude in the current, compared to the amplitude of the q-directed current. As the d- and q-axis in the figure suggests, the displacement of the rotor is 45 degrees from the αβ-reference frame in the example.

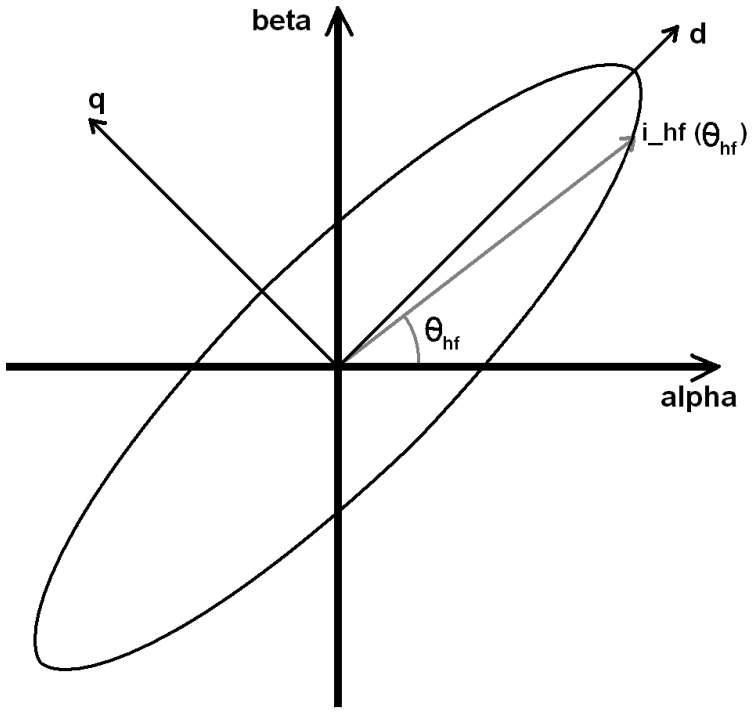

Figure 5-2 Current response with 45 degrees displacement of the rotor

Since the amplitude of the current response vector, i_hf(θ_{hf}) in Figure 5-2 is dependent on the angle of the high frequency flux vector, the current response can be used to establish the d-axis direction of the rotor.

To facilitate the position detection, the injected voltages and resulting currents are transformed from the stationary αβ-reference frame to a reference frame rotating with the injected frequency omega _hf. In Figure 5-3 the axis in the high frequency reference frame, from now on denoted as the hf-frame, are defined as x_hf and y_hf. The rotor displacement angle, θ_r in the figure, is still 45 degrees.

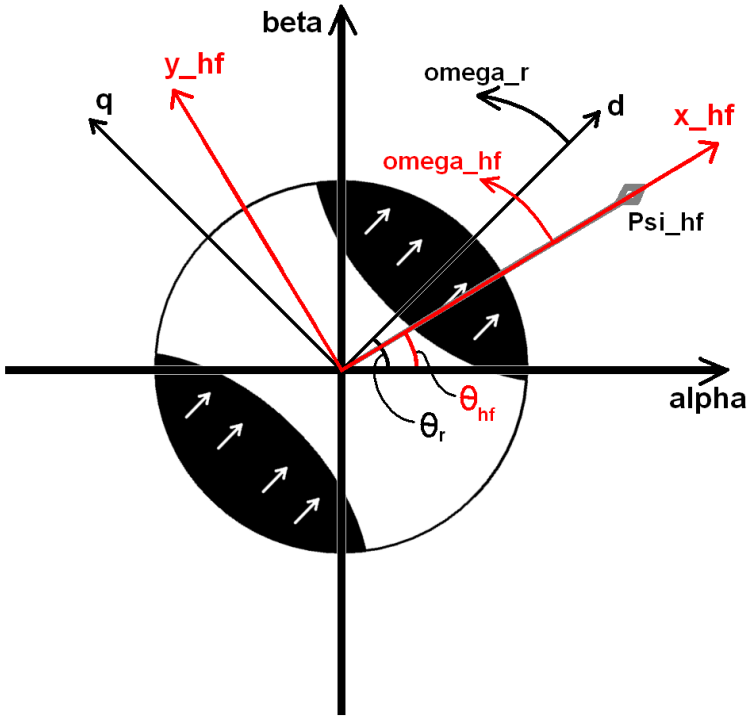

Figure 5-3 High frequency reference frame

As can be seen in Figure 5-3, x_hf is directed alongside the flux and from now on this is the definition of the hf-frame. According to the theory, the current and the flux will always be directed alongside each other, but due to the dissimilarities between the d- and q-directed reluctance this alignment will not always be true. The reason is that the d-component of the flux has to overcome a higher reluctance than the q-component and hence require a larger d-directed current component than a q-directed. If the flux vector for example is directed 45 degrees from the d-axis, i.e. built up by equally large d- and q-components, the d-component of the corresponding current vector has to be larger than the q-component. As a result, the current vector will have a smaller angle towards the d-axis compared to the angle of the flux. The consequence is that the current vector will lag behind the flux vector when the vectors are in the first and third quadrant of the dq-system, and lead when in the second and fourth quadrant. The only location at which the flux vector angle equals the angle of the current vector is when it consists of a d- or a q-component only, i.e. only when directed alongside the d- or the q-axis.

Seen from the high frequency reference frame, the current ellipse can be described as a dc-offset in the x_hf-direction, together with a part rotating at twice the speed and in opposite direction to the injected frequency. That is, for every lap the high frequency current carry out in the αβ-frame, the alternating part in the hf-frame completes two laps. This is shown in

Figure 5-4 where the left picture shows the high frequency current ellipse in the αβ-frame. The same instant is displayed from the hf-frame point of view to the right.

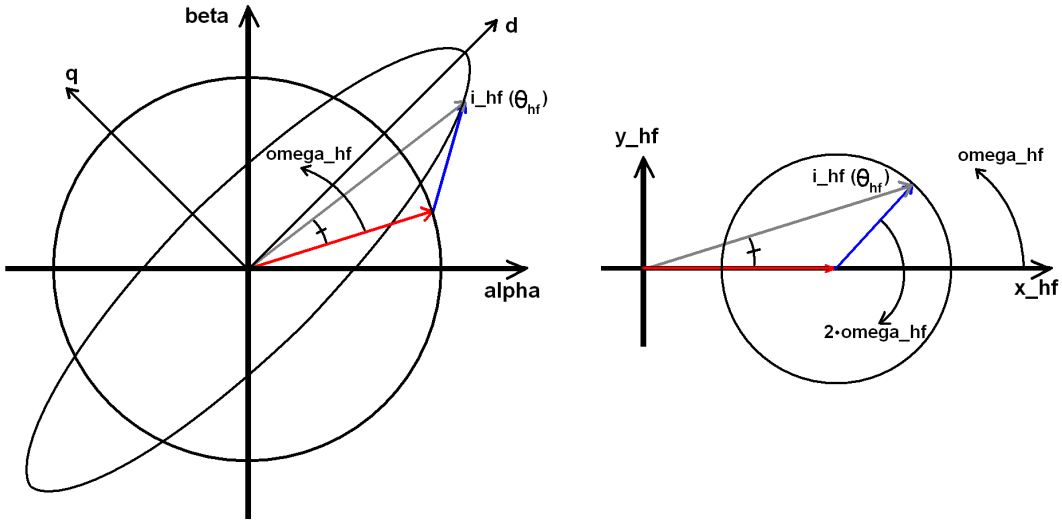

Figure 5-4 Current response in αβ- and hf-reference frame

As seen in the figures above, the pointy ends of the ellipse are directed along the d-axis, which coincides with the theory that the amplitude of the current, due to the higher reluctance, will be higher in that direction. This knowledge in combination with the knowledge of the angle in which the high frequency signal is injected at all time, gives an opportunity to decide the angle of the d-axis. When the amplitude of the current response is at a maximum, the current and therefore also the flux, will be pointing alongside the d-axis; hence the angle of the injected flux at that precise moment, equals the rotor angle at which the d-axis is directed.

Due to the fact that the rotor is symmetrical in positive and negative d- and q-direction respectively, the ellipse in the αβ-frame is symmetrical too; the maximum in the current amplitude returns twice each lap. Since *every other* maximum occurs when the high frequency current is directed opposite the d-axis it results in a 180 degrees misalignment every other time the requirements are fulfilled. The consequence is that the spatial saliency alone not will be enough to determine the polarity of the d-axis. To determine when the angle is correct or 180 degrees shifted, the saturation saliency has to be used.

If the rotor is configured so that the flux from the permanent magnets, Psi_m almost saturates the iron in the d-direction, there will be a noticeable difference in the reluctance whether the rotor flux is strengthened or weakened by the high frequency flux vector. The slight dissimilarity in the reluctance affects the inductance in the rotor, that is, the inductance will not only vary with the flux being in d or q direction, but also depending on if it is directed in positive or negative d-direction. This comes from the non linearity in the flux-current characteristics that is a result of the magnetic saturation which is principally shown in Figure 5-5.

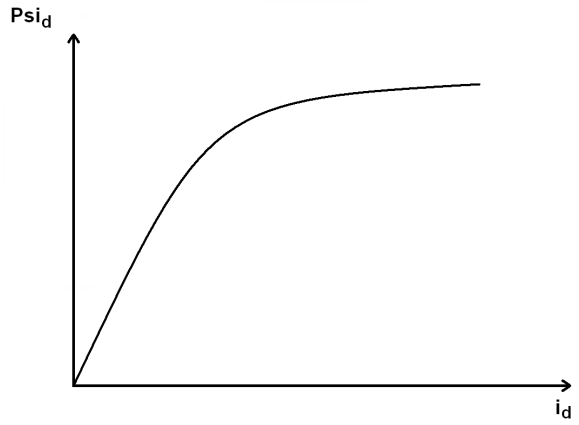

Figure 5-5 Flux-current relation

The extra axis, denoted as Psi_d* and i_d* in Figure 5-6 shows the flux at zero current, i.e. the flux originating from the permanent magnets. With a constant variation in the amplitude of the flux, delta Psi_d, the amplitude of the resulting current will be lower when directed in the negative direction. This is described in Figure 5-6.

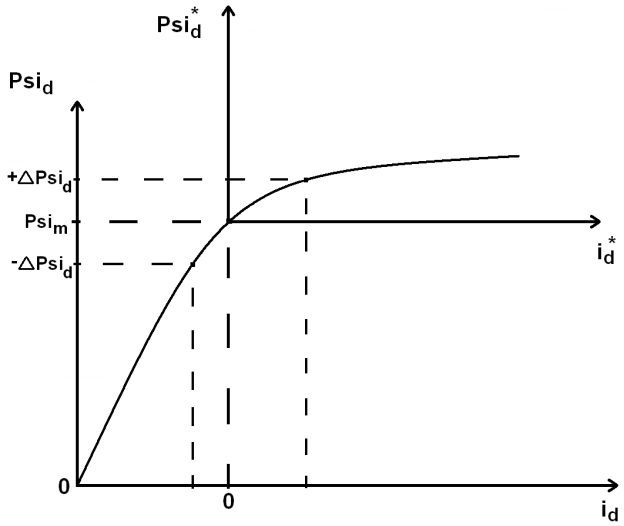

Figure 5-6 Flux-current relations with permanent magnet flux

The result is that the current ellipse will no longer be symmetric around the q-axis; the point directed in the negative d-direction will be more rounded compared to the end directed in positive direction. This case is explained in Figure 5-7 where the current vector will point in due order towards number one to eight and then back to one again and as can be seen, the vector reaches a local maximum in position one and five and a minimum at position three and seven. Hence the current vector is aligned with the q-axis at position three and seven and along the d-axis at position one and five.

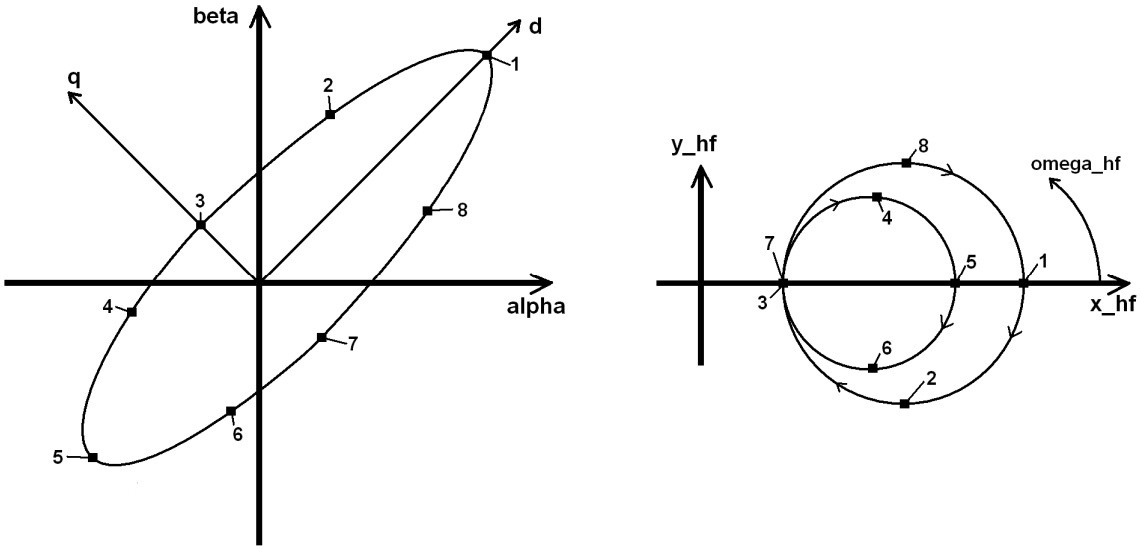

Figure 5-7 Resulting current response in αβ- and hf-reference frame

By detecting if the current vector reaches position one or five it can be determined whether the high frequency current vector is directed along the permanent magnet flux or reverse to it. This discussion suggests that the polarity of the magnets hence also the d-axis, is determined by looking at variations returning with half the frequency of the rotation in the hf-frame, i.e. at the injected frequency.

To summarize the method in general terms; a high frequency rotating voltage vector is applied to the machine inducing a rotating flux vector with the same frequency. The amplitude of the resulting current vector will be dependent on the inductance of the rotor. For each lap of the rotating flux vector it will be aligned with the d-axis two times, positive and negative direction, resulting in two current maxima. The current maxima will be slightly larger when the high frequency flux vector equals the direction of the permanent magnet flux, i.e. positive d-axis direction. This means that by detecting the largest current maxima for each lap of the high frequency flux vector, the rotor position angle can be updated at the same frequency as the injected voltage signal.

5.2.2 Implementation in Simulink

As mentioned above, the high frequency signal is injected as a rotating voltage in αβ-references at the output from the current regulator. Once that is done, all necessary information about the rotor position would in principle be possible to obtain by measuring the stator currents in combination with the known angle of the injected voltage. However, in order to get an accurate estimation of the angle, some additional modifications in the Simulink model needed to be done.

As the theory above implies, the information of the d-axis direction is found at twice the injected frequency and the polarity is determined with variations at the injected frequency. This was also confirmed with a Fast Fourier Transform (FFT) on the high frequency current in the motor. The FFT also revealed a dc-part in the current.

In order to isolate the useful frequencies from the switch frequency noise caused by the PWM converter, the measured current used for the position detection was low pass filtered; a band pass filter could not be used due to the dc-component. This meant that the fundamental currents, seen as disturbances by the rotor detection, where not filtered. Instead a feed forward of the reference current were utilized to subtract the fundamental currents from the measured

stator currents used in the rotor position detection unit. The cut off frequency on the filter was set slightly below half the switching frequency, well above twice the injected frequency where some of the information is received.

The transformation to the high frequency reference frame was implemented in a similar way as the well recognized Park-Clark transform which transforms quantities from αβ- to dq-reference frame, but with the angle of the rotating injected signal instead of the rotor angle. As is the case with the dq-transformation where the alternating currents in the αβ-frame are turned in to dc-quantities in the dq-frame, the transformation to an hf-reference frame makes it possible to consider the high frequency flux and currents as dc-components. The saliency based alternations are the only variations left.

The implemented low pass filters also cause a slight shift of the phase of the currents. As a result, the instant at which the angle of the flux vector is directed along the d-axis will not agree with when the filtered high frequency current is at its maximum, as the theory suggests. The result of this disagreement is an offset in the estimated angle. In order to compensate for this, a delay equal to the delay caused by the phase shift had to be added to the high frequency angle. With knowledge of the actual rotor position angle, the delay could have been adjusted until the estimation offset was reduced to nothing. But since the only knowledge of the angle in the final version would be the estimate, such a solution is not favourable. Instead a filter equal to that used on the currents where added to the high frequency angle signal going in to the rotor position detection, which reduced the angle offset to close to zero. A flow chart of the model including the sensorless rotor position detection is illustrated in Figure 5-8, further details can be found in Appendix B.

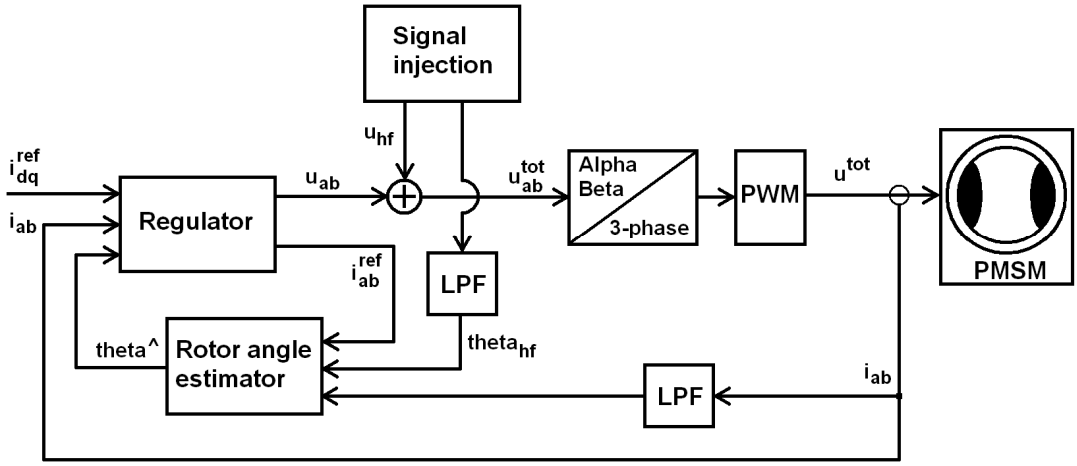

Figure 5-8 Flow chart of the model including the position detection

When implementing the method in Simulink it is important to have a non-linear model of the machine. Considering the theory; it can be clarified that the rotor position detection method would not be able to function properly if simulations where to be made using a traditional linear model of the motor. This as when using a linear model there would be no difference magnetizing the rotor in the positive or negative d axis direction. By defining the d- and q-directed inductances to different values, it would be possible to determine a direction of the d-axis, but it would not have been possible to determine the polarity.

6 Results of simulations in FEMM and Simulink

In the following chapter, the results from the simulations are presented. First the result from the simulations conducted in FEMM, followed by testing of the sensorless control method developed in Simulink

6.1 PMSM behaviour at electric loading

The results from the simulation of the principal design of the PMSM machine provided a first indication of the performance of the machine and how the different parameters changes when the electrical loading is increased.

First to be studied is the flux linkage dependency of the current applied in d and q axis. In a simple model of a PMSM this relation is linear and consists of the constant inductance L_d or L_q, as seen in Figure 6-1.

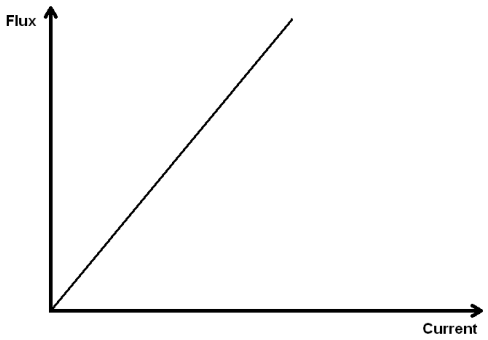

Figure 6-1 Relation between flux and current with constant inductance

Due to the irons properties it can not carry an infinite amount of flux. The almost linear relation between flux and current will start to change when the iron becomes saturated. It will require more and more current to increase the flux and the resulting relation will be similar to Figure 6-2.

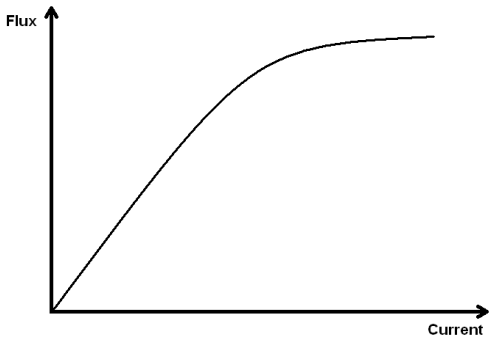

Figure 6-2 Relation between flux and current with saturation effects included

The real relation is however even more complicated and that is also what the results from the FEM-calculations showed. Figure 6-3 shows the flux linkage in the direct axis for different currents. The dotted circles in the figure represent the current density 5 and 10 A/mm^2 and is inserted to give an indication of the loading condition of the machine. To easier see the

amplitude of the flux the zero level is shown by the grey plane, the point with zero applied current is also marked with a black dot.

When the currents are set to zero there is already a d-axis flux in the machine due to the permanent magnets. Studying the change in flux when i_d is increased or decreased it is obvious that it is not a linear relation, this due to saturation effects in the iron. It can also be seen that the d-axis flux decrease because of cross saturation when a positive or negative i_q current is applied. This is expected as the d- and q-flux paths meet at two points which was shown in Figure 3-1.

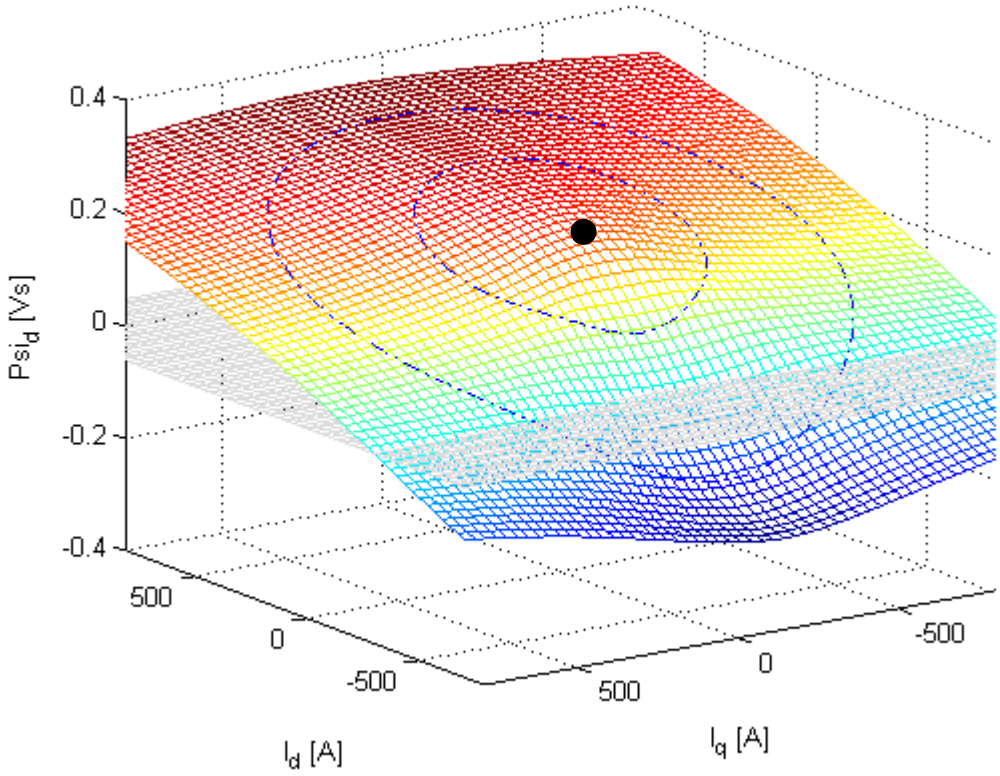

Figure 6-3 Flux in the d axis as a function of d and q axis currents

Looking at the q axis flux as a function of i_d and i_q in Figure 6-4 it is apparent that there are some differences to the d-axis flux. At zero current there is no q-axis flux as the permanent magnet flux only contributes to the d-axis flux. A similar non linearity between q-axis current and flux as for the d-axis flux can be seen though. At a first glance, the maximum of q-axis flux appearing for a negative i_d current can look strange. The maximum are however coinciding with the total demagnetizing of the permanent magnets. When the stator windings produce the same amount of d axis flux as the permanent magnet but with the negative direction the resulting d axis flux will be zero. This will make it possible for the q axis flux to fully utilize the shared part of the iron core and it will reach a maximum.

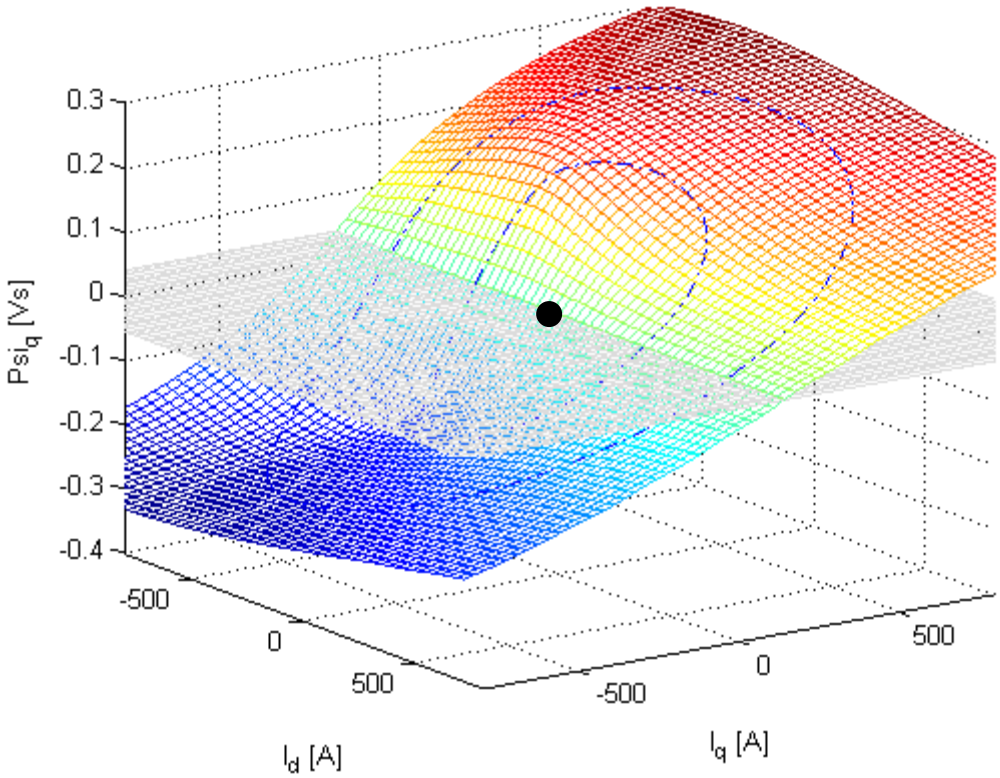

Figure 6-4 Flux in the q axis as a function of d and q axis currents

This demagnetization can also be seen in Figure 6-5 that is the total flux in the machine. The bottom of the cone is the operation point where no q axis current is applied and hence there is no q axis flux, and the d axis flux from the stator created by the negative d axis current entirely cancels the flux in the d axis direction.

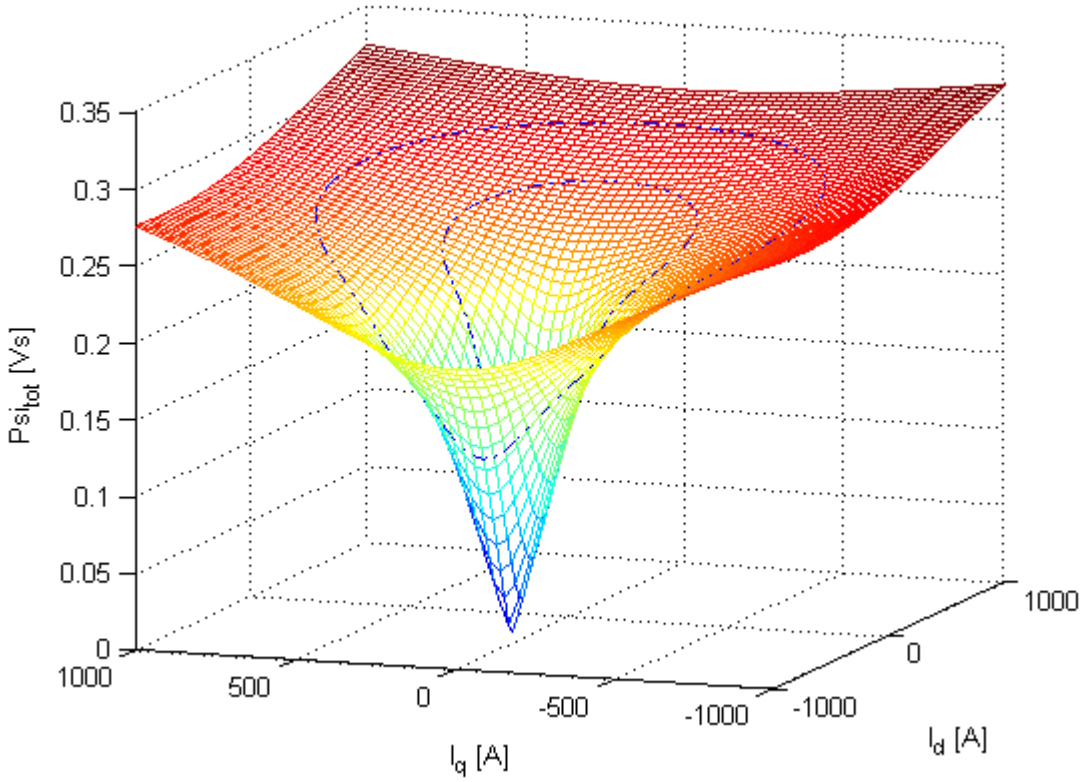

Figure 6-5 Total flux in the machine as a function of d and x axis currents

When establishing the optimal control strategy for a salient PMSM machine it is found that to get maximum torque it is usually advantageous to apply some negative i_d current in addition to the positive i_q current. By this the reluctance torque is utilized. As can be seen in Figure 6-6 a large part of torque in the simulated geometry comes from reluctance torque; the torque is increased for a constant i_q when negative i_d is applied, i.e. when the PM-flux is weakened. A maximum is reached when the magnets are completely demagnetized. This is though not a possible working condition for the machine as the magnets are likely to be destroyed and the machine rendered useless.

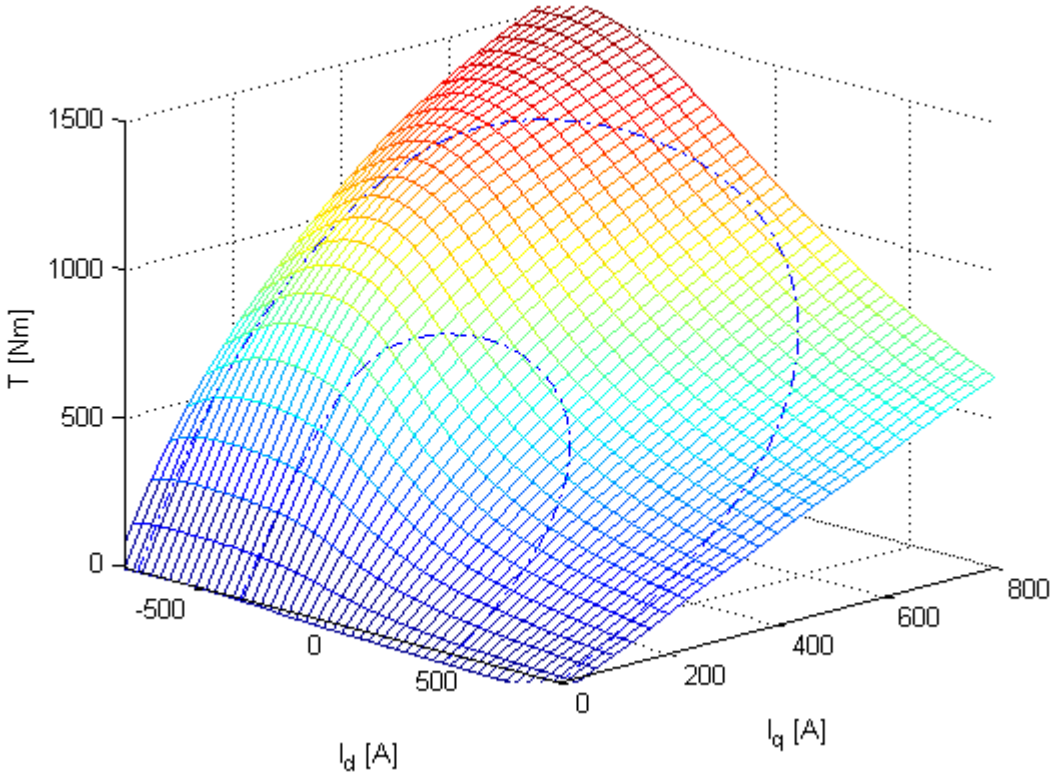

Figure 6-6 Torque as a function of d and q axis currents

That the PMSM develops large reluctance torque is a big advantage in HEVs where a large constant-power speed range is preferable. Toshiba even calls there machine with similar configuration a Permanent Magnet Reluctance Motor [33].

Similar machines are also treated in [34]. A prototype IPMSM with a saliency ratio between the d- and q-direction of 5 has a torque production where over 70% comes from reluctance torque; this gives a constant-power speed range up to 5:1.

6.2 Sensorless rotor position detection in Simulink

To verify the functionality of the implemented sensorless control method, testing at different loading conditions where performed. Before these tests could be performed, the functionality at no load had to be confirmed.

6.2.1 Sensorless rotor position detection at no load conditions

A plot of the high frequency stator flux rotating in the αβ-frame can be seen in Figure 6-7 where the constant amplitude forms a circle.

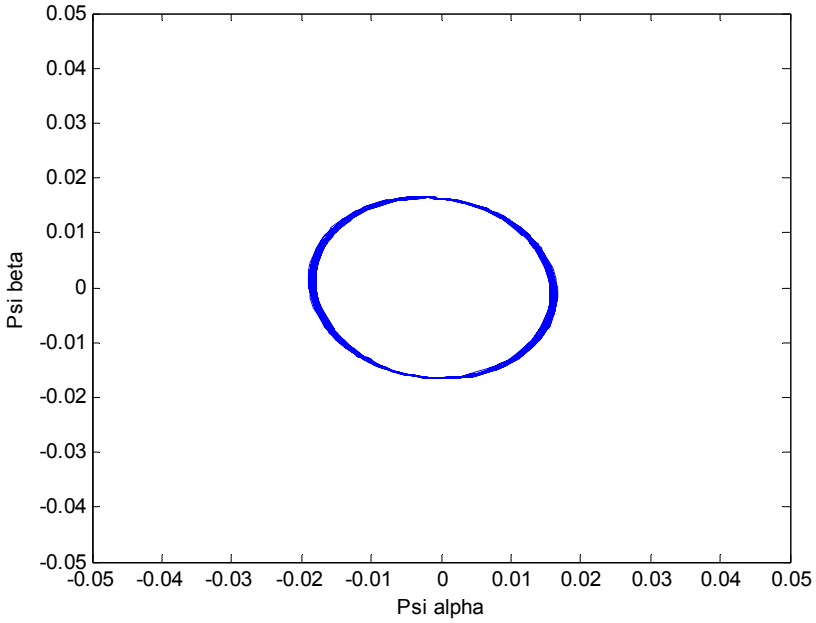

Figure 6-7 Rotating stator flux linkage with constant amplitude

The resulting current response in the αβ-reference frame when the d-axis is deviating from the α-axis with 45 degrees is presented in Figure 6-8 where an egg shaped ellipse with one end more pointed than the other is formed. As described in the previous chapter, this makes it possible to detect not only the d-axis, but also the magnetic polarity of the pole i.e. the direction of the d-axis.

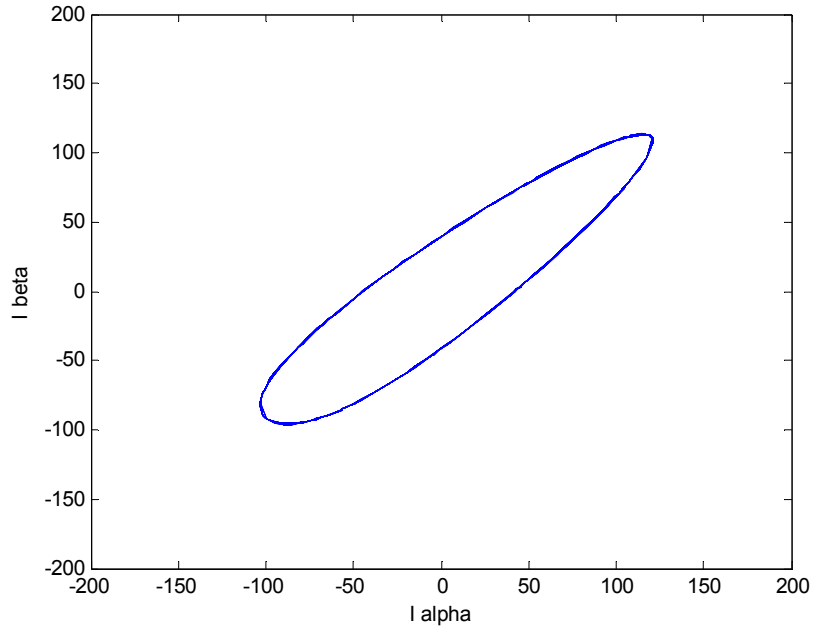

Figure 6-8 Resulting current response in the αβ-reference frame at no load

The current response transformed to the high frequency reference frame is plotted in Figure 6-9. Two circles are formed with a dc-offset in hf_x direction; the bigger circle is when the

current vector contains a positive d-component and the smaller circle when the d-component of the current is negative. When comparing the plots in Figure 6-8 and Figure 6-9 with the current response in the αβ- and hf-reference frame in Figure 5-7 it can be determined that the implemented method agrees with the theory.

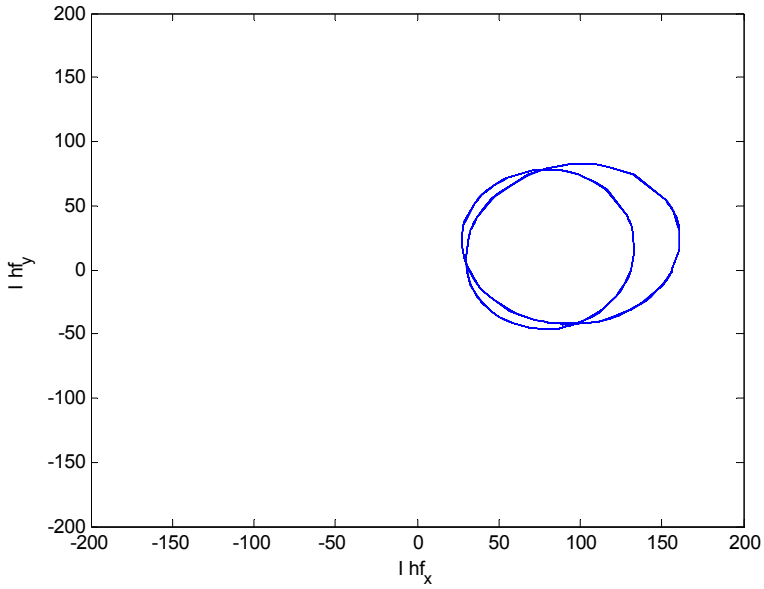

Figure 6-9 Resulting current response in the hf-reference frame at no load

The hf-currents as a function of time are shown in Figure 6-10. As can be seen, the imaginary part of the current response, i_hf_y is shaped like a sinus wave around zero, while the real part, i_hf_x has a dc offset that displace the current from zero. It can also be seen that every other peak of the hf_x current is a bit higher compared to the previous peak. This maximum occurs at the instant when the rotating hf-flux and current vectors are directed along the d-axis. The local maximum between the peaks is when the hf-vectors points in the negative d-direction while a minima in the hf_x current identifies the q-axis.

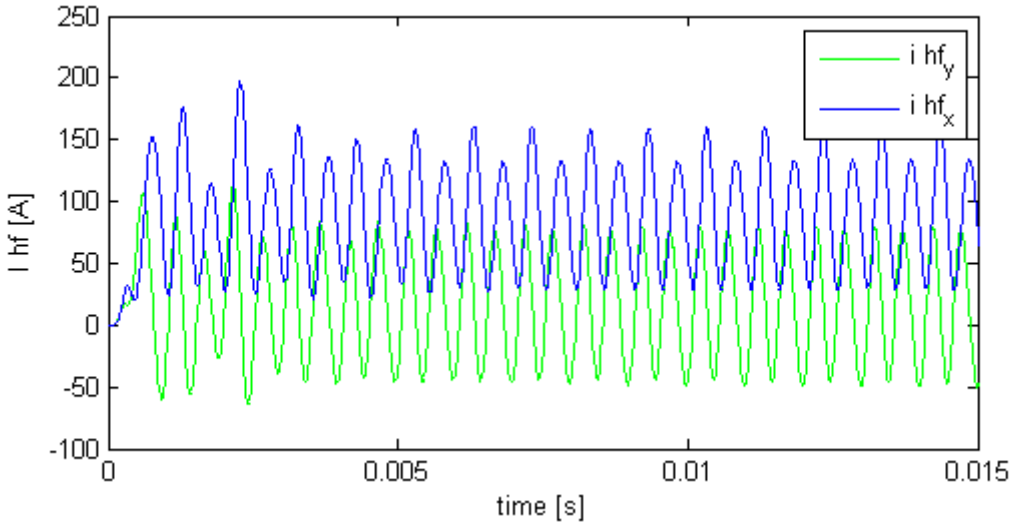

Figure 6-10 Hf-current response as a function of time

In Figure 6-11 it is explained how this knowledge can be used to detect the angle. The upper plot shows the current response from Figure 6-10 and in the lower plot the high frequency angle is plotted from -180 to +180 degrees, during multiple hf-flux vector revolutions. The dotted line combining the two plots shows that at a higher peak, the hf-angle equals the real angle, while a lower peak means that the hf-angle are 180 degrees misaligned to the d-axis. In the plot, the real angle is located 45 degrees from the α-axis, which means that the sampled angle will be incorrect at the beginning, before it aligns with the real angle after approximately 2.5 ms.

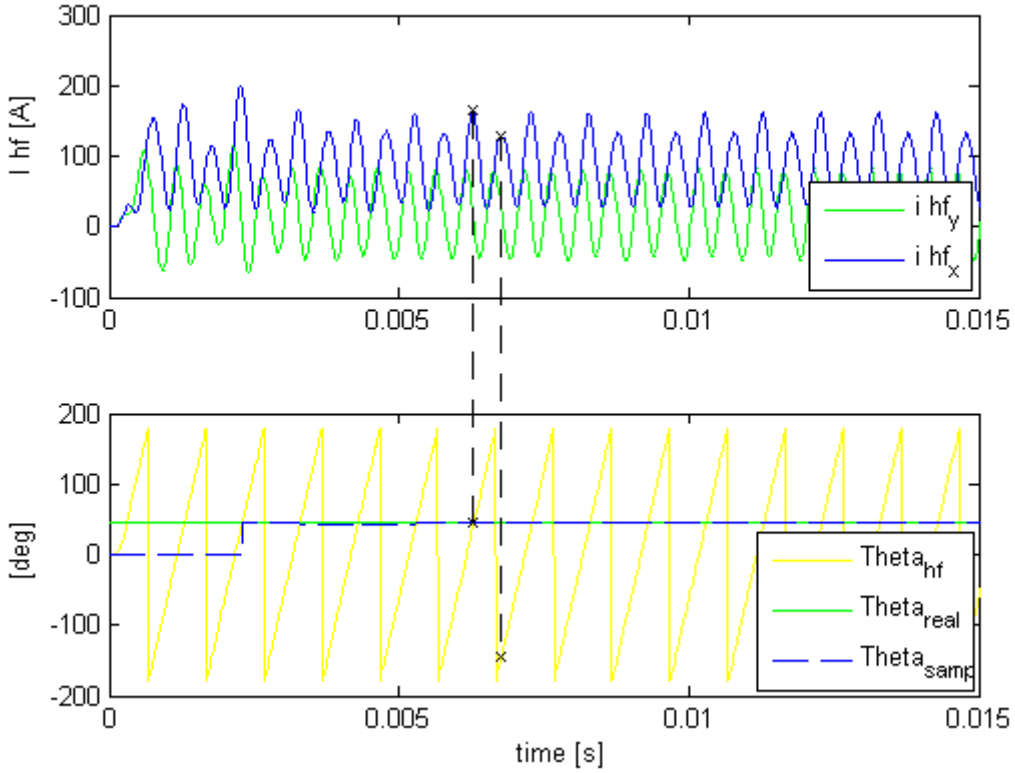

Figure 6-11 Rotor angle estimation

Since it can be determined by looking at the current response at what instant the rotating flux vector is directed in positive d-direction, the angle of the injected signal at that instantaneous moment can be used as a substitute to the real angle. This means that the sampled angle will be updated once every lap, hence with the injected frequency. The result will be that the sampled angle will be able to follow the real one even when the rotor rotates, i.e. when θ_r increases, as in Figure 6-12.

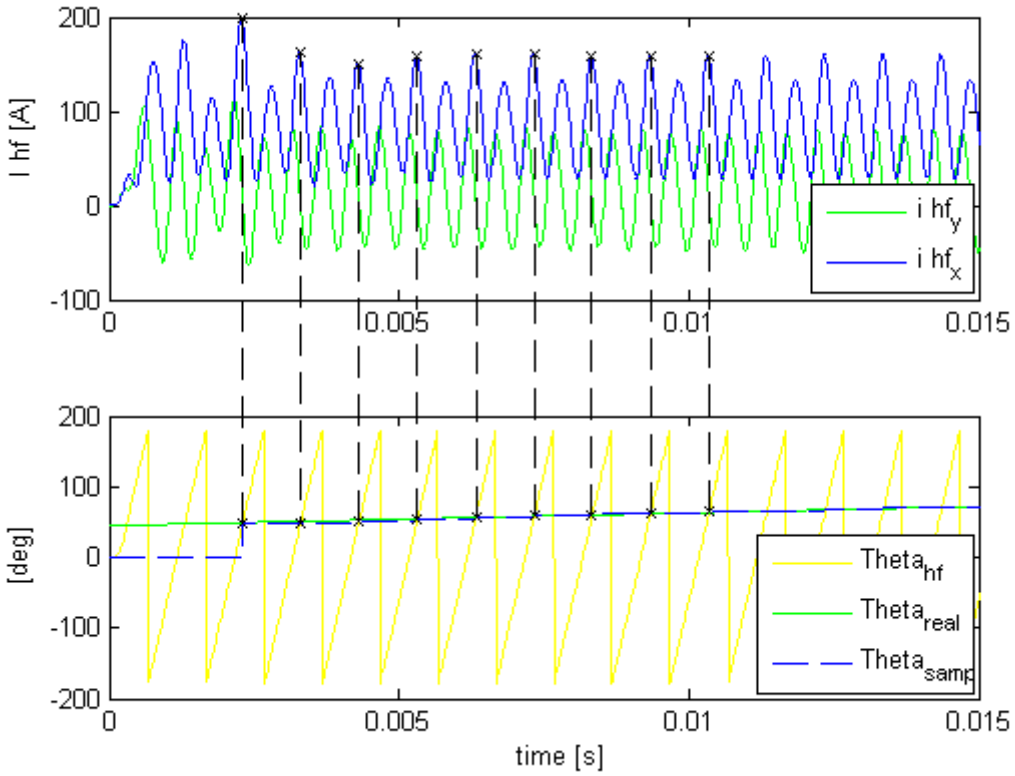

Figure 6-12 Rotor angle estimation at 5 electrical Hz

By plotting the difference between the real and the sampled angle, it can be determined how well the angle estimation method works. This is done in Figure 6-13, where the real rotor angle is plotted in the upper figure, while the angle estimation error is plotted underneath it. After 20 ms the rotor is rotated with 5 electrical Hz by an external force making the rotor angle to change from 45 degrees at start, up to 80 degrees 20 ms later. In the lower plot it can be seen that the error starts at 45 degrees. Once the hf-currents have been stabilized, the rotor position can be estimated and after about 2.5 ms, the angle error is reduced to close to zero. The angle error signal becomes noisy when the rotor starts to rotate after 20 ms, but stays at around zero degrees.

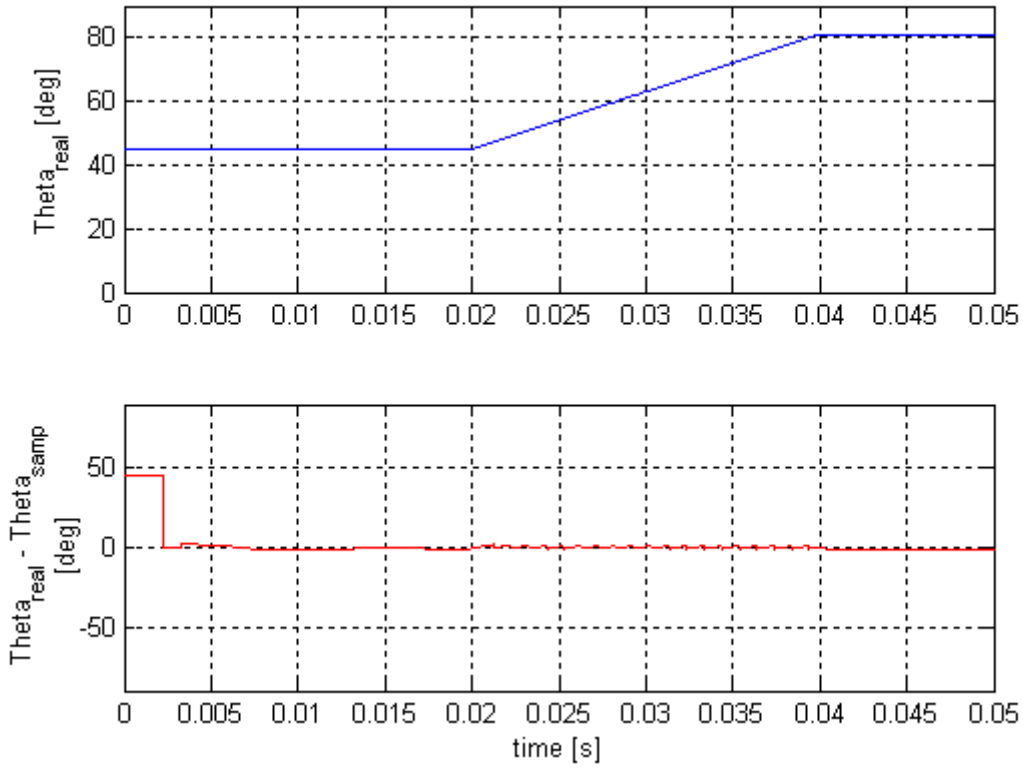

Figure 6-13 Real angle and angle estimation error without load

The noise on the angle error signal is originating from the fact that the estimated angle is updated with the injected frequency, i.e. the estimated angle will be constant during one high frequency period. This will cause the estimated angle to fall behind the real angle until the next angle estimation update occurs. This is displayed in Figure 6-14 where the estimated angle tends to look like a discrete signal, causing the angle error to form a saw tooth wave while the rotor rotates. As in Figure 6-13, the rotor starts to rotate with 5 electrical Hz at 20 ms and stops 20 ms later.

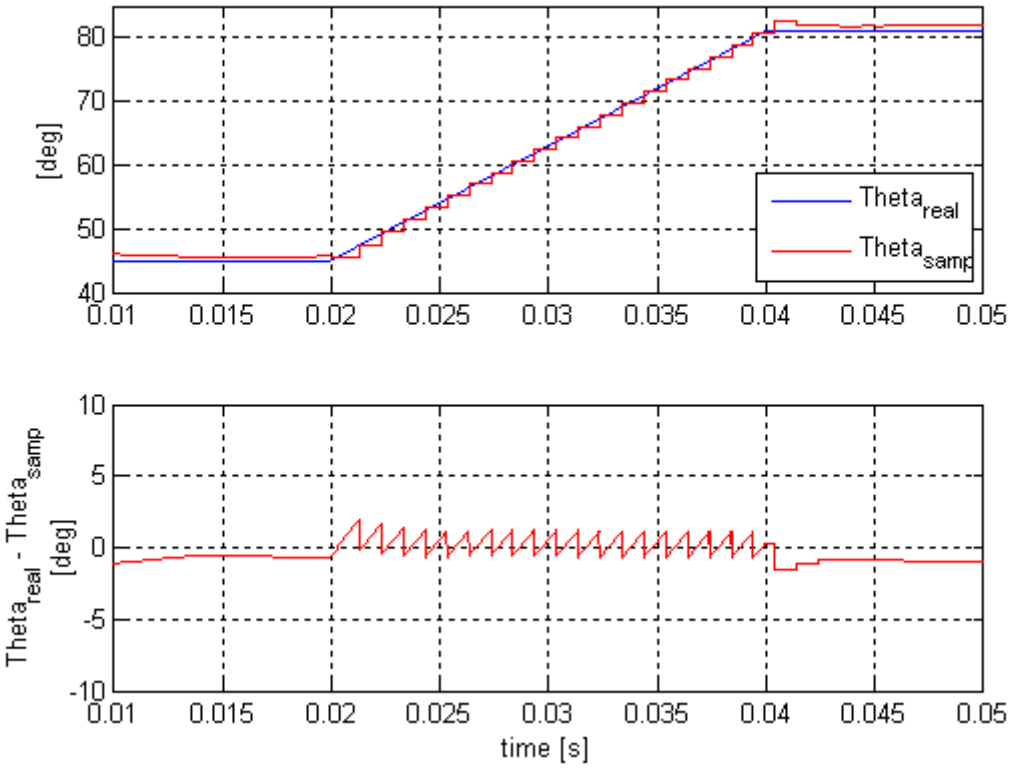

Figure 6-14 Real and estimated angle and angle error without load

Considering how the plots agrees with the figures in chapter 5, explaining the theory, in combination with the low angle error in Figure 6-13 it can be determined that the rotor position estimation works satisfactory at no loading conditions.

6.2.2 Sensorless rotor position detection at loading conditions

With the method working according to the theory for no load conditions, it had to be tested with loading currents applied, something that proved to mean problems with the sensorless rotor position detection method.

In Figure 6-15 two torque producing q-current reference steps of 200 A is applied after 20 ms and 60 ms respectively. The d-current reference is kept constant at 0 A. After 0.1 s the q-reference current is reduced to zero again. As can be seen in the middle and lower plot, showing the real and estimated angle and the difference between the real and the estimated angle respectively, the deviation is 45 degrees until the correct angle is detected and the angle error is reduced to close to zero after about 2.5 ms.

At the time of the first current step, disturbances in the angle detection occurs; the angle error signal becomes disrupted for almost 10 ms before it become constant again. Once the signal is stabilized, the estimated angle disagrees from the real angle, shown in the middle plot, resulting in a stationary angle error in the lower plot. The same procedure is repeated when the q-current is increased to 400 A, the estimated angle is disturbed and when returning to a stable condition, an even larger stationary offset can be seen. When the current demand is set to zero again, the sampled angle estimation is interrupted for some time before it is stabilized again, this time around the real angle. Hence, problem with the rotor position detection occurs

at rapid changes of the torque producing currents and at heavy loading conditions but when the current is decreased, the real angle is established again.

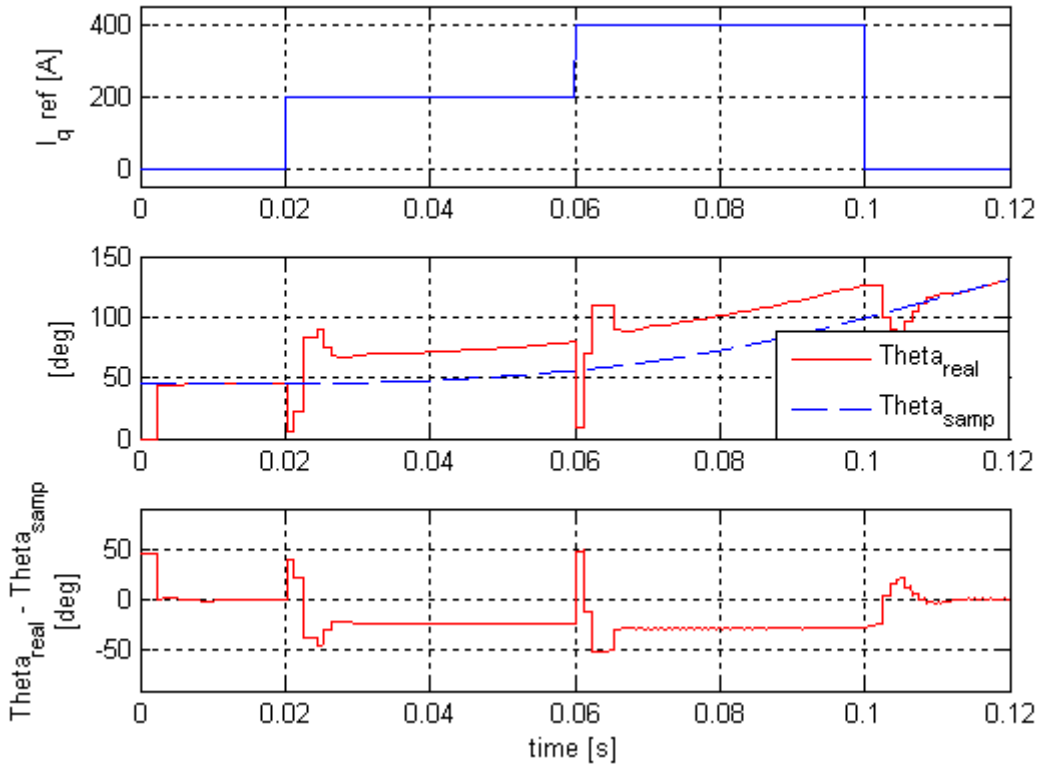

Figure 6-15 Disturbances with current steps

In Figure 6-15 it can also be seen that at steady state conditions, the estimated angle do not drift away any further, it is kept constant around a certain angle even though it no longer agrees with the real angle. The offset also tends to be dependent on the applied current; a higher current demand gives a higher angle offset and once returning to no load conditions, the detected angle agrees with the real one again. This behaviour suggests that the method still can detect *an* angle even though it not is the correct angle.

To summarize the simulation results from Simulink, the estimation method seams to work properly at no loading conditions, but it seam to lose its angle detection ability for some time when rapid changes in the reference current is applied. Further more, an incorrect angle is detected when a torque producing current is applied, but since the erroneous angle is constant for a constant current, an angle is still being detected but with an offset to the real angle. This offset also seams to be dependent on the amplitude of the current demand; zero current means no offset while high current and loading demands gives an angle error, increasing with increased torque producing currents.

7 Analysis and optimization

7.1 Saturation effects

The results in chapter 6 showed that difficulties occurred in the sensorless performance and that they where related to high current demands. The fact that an increase in current meant an increase in the angle offset suggests that it is the saturation effects when the machine is loaded that causes the problems. Since it is desirable to fully understand this problem and find possible ways to compensate for it to achieve enhanced sensorless performance the phenomenon is studied further in the following chapter.

7.1.1 Theory

Since an angle, even though it is an incorrect one, still is detected when the machine is heavily loaded together with the fact that the method detects the d-axis by detecting the direction of the hf-current vector maxima, it can be proposed that the highest current vector no longer is in parallel with the PM flux linkage. This would mean that the tip of the ellipse no longer is directed in d-direction, thus that the hf-current ellipse in the dq-frame has turned away from the d-axis. The change of the maximum hf-current vector direction, i.e. the turning of the ellipses in the dq-system indicates that the maximum and minimum reluctance no longer is aligned with the d and q axis.

When the supplied fundamental current to the machine is zero, the maximum reluctance in the rotor is in the d axis direction and the minimum in q axis direction. As the machine is unloaded there exists almost no cross saturation effect. A rotating flux vector with constant amplitude applied to the machine consists of sinusoidal variations of the d and q axis flux displaced 90 electrical degrees. As there is almost no cross saturation, i_d is dependent on the d-axis flux and i_q is dependent on the q-axis flux. Consequently, the maxima and minima of the d- and q-axis currents coincide with those of the flux, e.g. the current is in phase with the flux. This is illustrated in Figure 7-1. Due to the fact that the reluctance in d direction is higher than in q direction, i_d will have larger amplitude and the current therefore constitutes of an ellipse in the dq current plane.

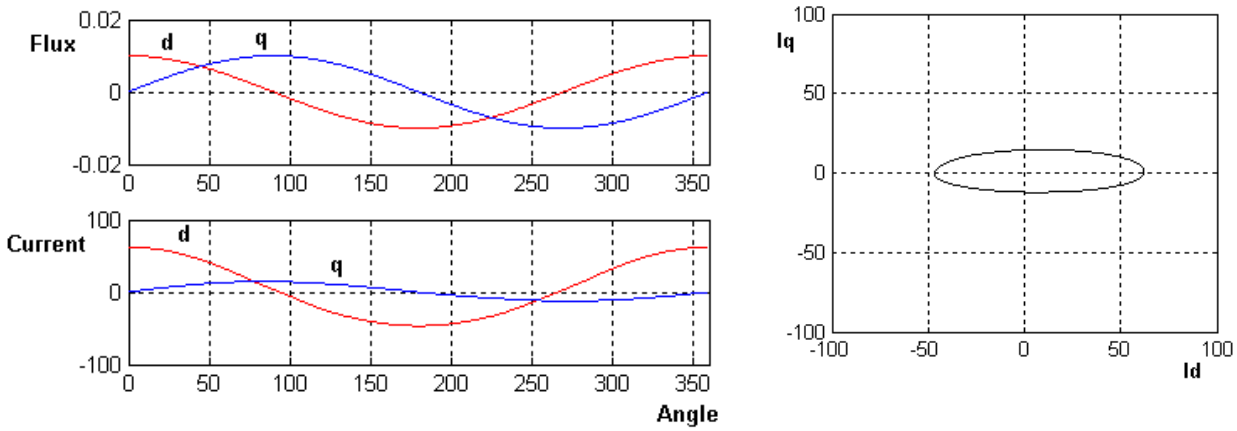

Figure 7-1 High frequency flux and current in phase with zero fundamental current applied

When the fundamental current loading increases the cross saturation effect will be more and more eminent. To understand how this affects the ellipses an example of i_d as a function of d

and q axis flux is shown in Figure 7-2 and Figure 7-3. The circles shows the rotating high frequency flux vector applied by the sensorless system during four working conditions; i_q=0, 200, 400 and 600 amps respectively while i_d is kept constant at 0 A. Hence, higher i_q current means that the circles are moved along the positive flux q axis.

For better visualization the amplitude of the high frequency flux is increased, making the current response ellipsis larger which makes the details easier to study. The cross saturation effect can be seen for the higher working conditions, where also the q axis flux affects the amplitude of the i_d current.

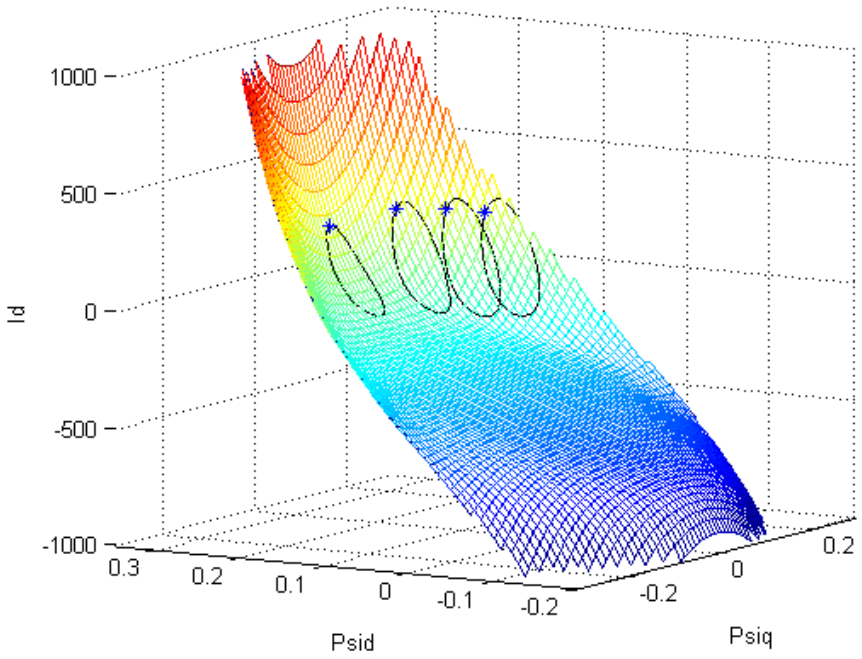

Figure 7-2 I_d current as a function of d and q axis flux, view 1

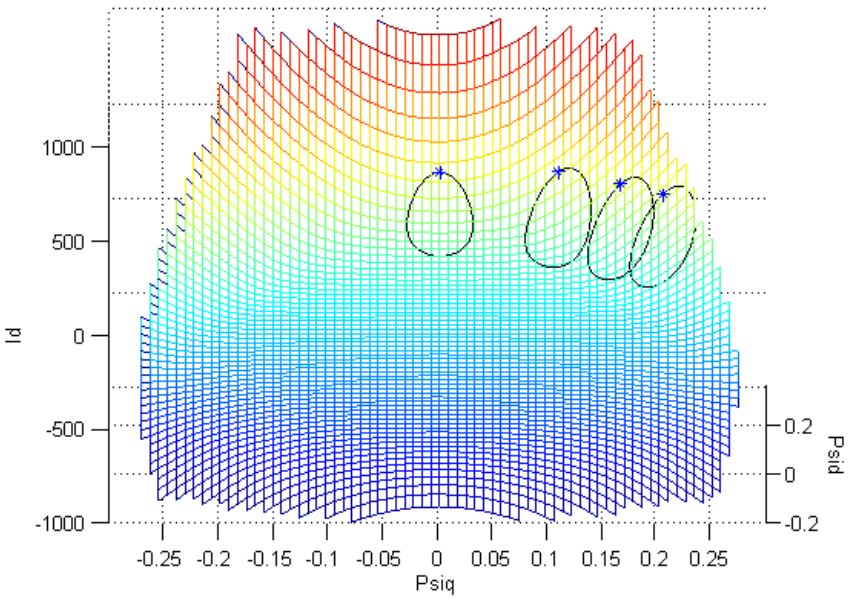

Figure 7-3 I_d current as a function of d q axis flux, view 2

The star at the high frequency flux circles in the figures indicates the point where the d-axis flux reaches its maximum. At higher current levels it is evident that the maximum and minimum i_q do not coincide with maximum and minimum q-axis flux. Instead maximum i_q occurs when the q-axis flux is slightly lower than maximum but also some d axis flux is applied. In the same way the minimum i_q occurs when some negative d-axis flux is applied. The same phenomena exist for the d-axis current which makes all the maxima and minima of the currents displaced from those of the fluxes. Hence, the current is no longer in phase with the flux. Figure 7-4 illustrates this; it is the displacement from the d- and q-axis that creates the turning of the ellipses.

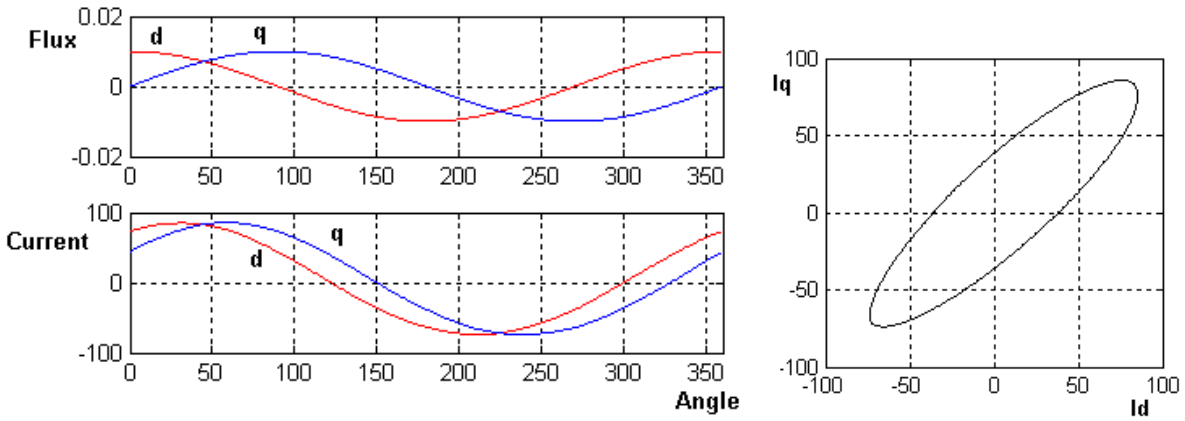

Figure 7-4 High frequency flux and current with fundamental current applied

Since the problem is caused by the cross saturation it gets more and more prominent as the fundamental current increases, the direction of the highest reluctance will turn more and more towards the q axis.

If a considerable large i_q current is applied a reduction in i_d will cause an additional turning as the cross saturation effects then increases. This could be seen in Figure 7-2 and Figure 7-3, when the d-axis flux is reduced the i_d current surface bends more due to the cross saturation.

The direction of the highest reluctance is hence the direction of the highest current response from the high frequency rotating flux vector applied in the used sensorless method. According to this, the dq-system aligned according to the estimated direction will cause a stationary offset to the real angle, dependent of the applied current. This means that at high torque output there will be a large angle offset. As the offset is constant for a certain current, it would be possible to compensate for it. Still, even if it would be possible to compensate for the cross saturation to a full extent, the problem with regular saturation would still remain though: A large i_q causes saturation meaning that the reluctance along the q axis will increase. If the q-axis flux path is saturated so that the reluctance is decreased to the same magnitude as the d-axis reluctance, the current response from the rotating flux vector will begin to equal a circle. This would mean that the reluctance would become the same in all directions in the dq-plane; hence it would be impossible to determine a direction. The problem with regular saturation when no cross saturation exists is illustrated in Figure 7-5. Ellipse number one symbolize a ratio between the d- and q-inductance of about five, ellipse number three a ratio of about one.

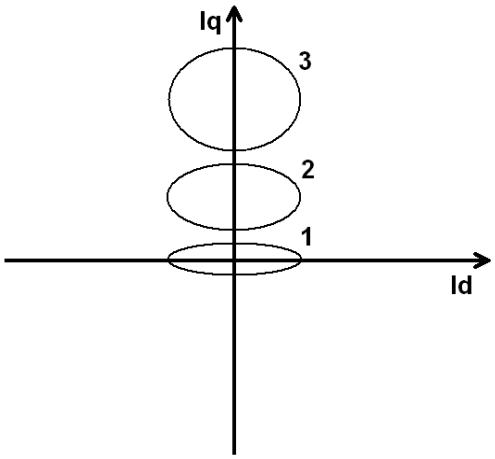

Figure 7-5 Illustration of saturation

To avoid the problem there should be a large difference in inductance from the start and the q axis flux path should not be easily saturated.

If no cross saturation effect would exist, the angle would be possible to determine without offset as long as there is a measurable difference of the d- and q-inductance and L_d is larger than L_q.

To establish if it is possible to use the sensorless method on a machine with cross saturation effect at a specific electrical loading, it is important to compare the ratio of the minimum and maximum dynamic inductance in the *entire* dq-plane rather than the ratio between the d- and q-directed dynamic inductances. In Figure 7-6 the current response from a rotating flux vector with constant amplitude at loaded condition is shown. As the amplitude of the flux is constant, the dynamic inductance is inversely proportional to the current amplitude, $L = \psi / i$. The ratio

between current amplitudes can therefore be used to determine the ratio between the dynamic inductances.

When the machine is unloaded the ratio between the dynamic d- and q-directed inductances is large, but in the loaded condition it is however reduced to close to one due to the turning caused by the cross saturation. The loaded condition can be seen in Figure 7-6 where the arrows indicate that the inductance would seem to be the same in d- and q-direction. But as can be seen, the current response does not form a circle, meaning that the ratio between the minimum and maximum dynamic inductance in the dq-plane can still be considerably large if the inductance is measured when the current vector is built up by both a d- *and* a q-component. This makes it possible to determine an angle also at loading conditions and if the offset between the angle and the d axis is known for a certain applied current, the real rotor flux angle can be calculated. That is also why it is possible to get a considerable amount of reluctance torque even though the ratio between the d and q dynamic inductance is low.

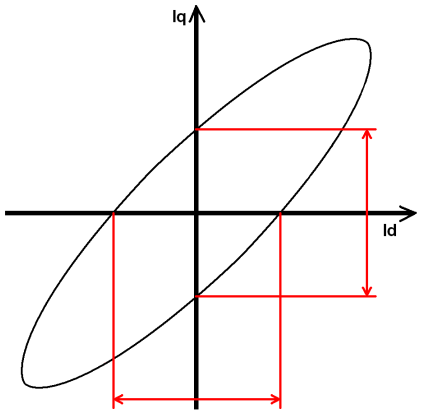

Figure 7-6 The high frequency current response with marked d and q axis current

But if the ratio between the minimum and maximum dynamic inductance in the dq-plane too gets close to one, the current response will form a circle in the dq-plane, making it impossible to determine any angle whatsoever.

The problems originating from the saturation should be the same for most sensorless control methods as they all utilizes the saliency in the rotor to determine the position. The ability to directly determine the correct rotor position will be lost when the properties changes with electrical loading as shown.

7.1.2 How the saturation affects the sensorless performance

In Matlab different control strategies can easily be tested, e.g. different ways to choose the dq-currents when increasing the torque can be performed. For the rotor configuration used in the simulations, it is stated in Chapter 6.1 that some amount of negative i_d is advantageous to achieve higher torque utilizing the reluctance torque. In Figure 7-7 three different control strategies are shown, each one following one of the three lines connecting the hf-current response ellipses. The different reference current approach is built up with different amount of negative i_d in addition to i_q. As can be seen, the strategy farthest out to the left in the figure; the one with most negative i_d applied is the one that suffers most from the displacement from the dq-axis. This due to that the cross saturation is more evident when current is applied in both d- and q-direction.

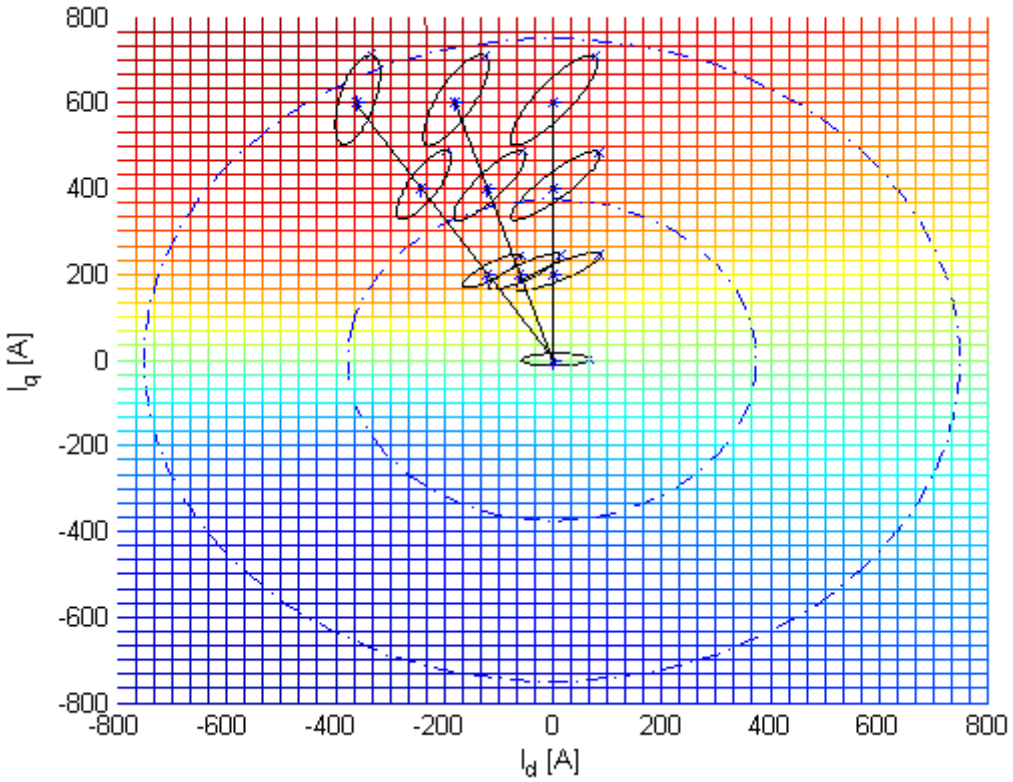

Figure 7-7 High frequency current response ellipses from three different control strategies

Even though a large angle offset occurs, the control strategy with most applied negative i_d is not necessarily the inferior one. When a negative d current is applied, the reluctance torque is acquired in addition to the electromagnetical torque. By making use of the reluctance torque, the required torque is attained at a lower absolute current level. The difference in torque creation capability can bee seen in Figure 7-8 where the total amount of torque is increased when the amount of negative d current is increased.

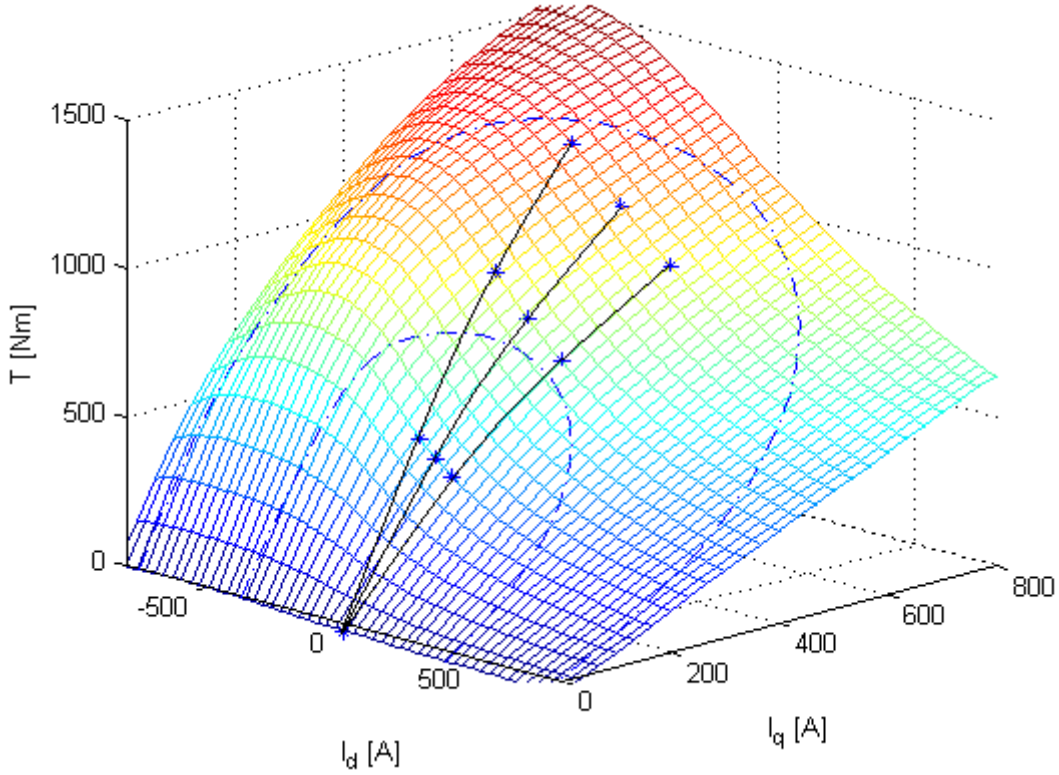

Figure 7-8 Torque from the three different control strategies

How the inductance changes in the dq-plane and consequently makes the ellipses turn seems to vary greatly for different amount of applied current. To get a better understanding of this change and if there is any working conditions that should be avoided the whole dq-plane should be investigated. In Figure 7-9 the current response from high frequency rotating flux vectors all over the dq-plane can be seen. The small x on the ellipses represents the maximum hf-current vector direction; hence the direction of the estimated d axis. As can be seen, this estimation agrees with the real direction when the machine is unloaded, i.e. when i_d and i_q equals zero.

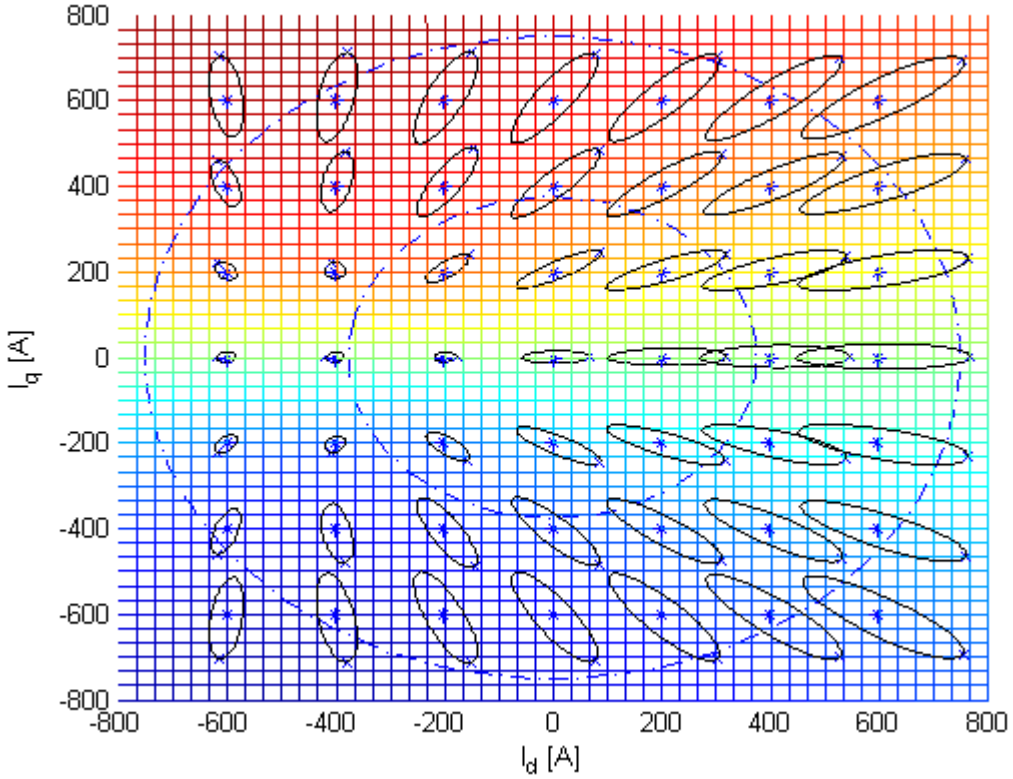

Figure 7-9 High frequency current response ellipses in the whole dq-plane

The figure above represents the problem with saturation very well. How much the direction of maximum reluctance deviates from the d axis is represented by the turning of the ellipses in relation to the d-axis and is caused by the cross saturation. The proportion of the ellipse indicates how difficult the detection of the direction will be. If the ellipses are almost circular, e.g. the ratio between length and width is small; the detection will be hard considering possible noise in the measuring equipment if implemented in a real control system. Consequently, conclusions can be drawn from Figure 7-9 about the direction of lowest dynamic inductance in the rotor and how difficult it will be to detect, in all working conditions for the machine. This is important information when developing the control strategy for the machine. To accomplish high efficiency it is desirable to find a strategy that develops the wanted torque with shortest possible current vector. In Figure 7-8 it could be seen that this is when combining positive i_q with some additional negative i_d, this however gives large angle offset according to Figure 7-9. It therefore seems difficult to combine high efficiency and small angle offset in a control strategy. The best approach would then be to choose a strategy with high efficiency and try to compensate for the offset. This should be possible as long as working conditions where there is a small difference between the maximum and minimum reluctance is avoided. In Figure 7-9 it can be seen that problem occurs at a very high negative d current; the high frequency response will constitute a circle instead of an ellipse. This is however a working condition that is not allowed due to the risk of demagnetizing the permanent magnets.

7.1.3 Compensation

Knowing the extent of the saturation effects and how it influences the performance and ability to sensorless control the machine, it would be desirable to find a strategy to compensate for the unwanted behavior.

7.1.3.1 Look up table

The most straight forward approach to compensate for the angle deviation where the cross saturation causes the maximum reluctance axis to turn would be to establish a look up table. This can be done by calculating or measuring the angle deviation for the currents in d and q axis from zero to maximum in appropriate steps. A problem with this method is that the angle deviation is dependent on the current vector applied to the machine at that moment. This means that the rotor flux angle has to be known to be able to compensate for the deviation. Normally this is not a problem as the angle is determined correctly at start up when no torque is applied; the correct angle can then be kept with help of the look up table when the electrical loading increases. Problem arises if the correct angle is lost due to for example disturbances at some point and the current vector applied to the machine might be another than what was intended. A control system using this type of compensation method would still use the compensation angle for the intended angle and the error could escalate.

These kinds of errors in the estimated angle will hopefully be detected in a real control system, by for example comparing the reference torque with the torque output. It will unfortunately not be possible to recover from a problem like this; the only option would be to back down to zero torque and reinitiate the rotor flux angle.

The angle error for a large part of the dq-plane was calculated in Matlab with the results originating from FEMM. A surface plot of the angle offset at different currents could then be made. In Figure 7-10 this deviation can be studied and shows the increase with rising positive q-current and negative d-current.

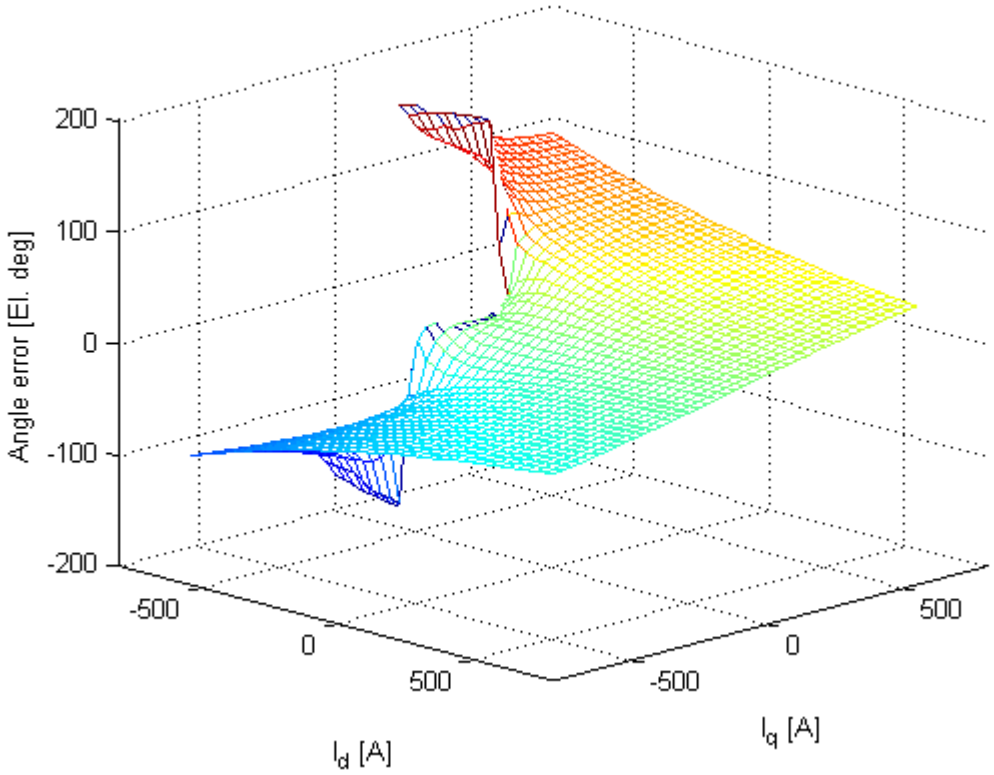

Figure 7-10 Angle error as a function of d and q axis current

This information was exported and implement in Simulink as a look up table. The performance of the sensorless control system was then considerably increased. Figure 7-11 shows the angle error with and without the compensation at i_q equal to 400 A, producing approximately 900 Nm of torque in the simulated machine.

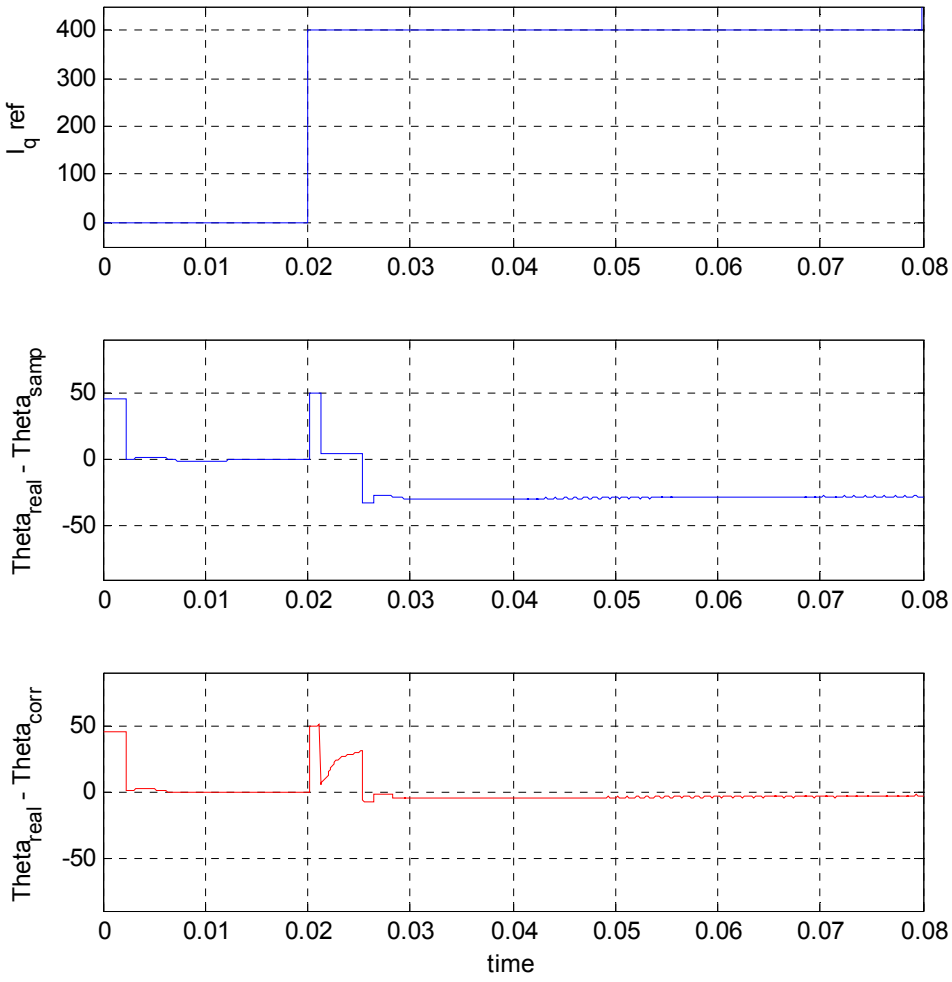

Figure 7-11 Angle error at iq= 400 A without and with compensation

To implement the described compensation method for a real machine the data can be retrieved from measurements of the stator flux linkage as a function of currents. The theoretical angle deviation can then be calculated.

However, the problems when losing the angle remain, making this method an unreliable alternative.

7.1.3.2 Compensation method independent of previously rotor position information

Some effort has been spent on developing a compensating method that does not rely on previous information about the rotor angle to perform the compensation.

If the angle is lost with the previously used method the only information about the applied current is the length of the current vector. This makes it impossible to use the look up table if the angle is unknown.

In Figure 7-9 ellipses were plotted for multiple currents in the dq-plane. It could be seen that both the proportions and direction of the ellipses changed in the plane. At a certain current level resulting in a circle with constant radius in the dq-frame, the direction and proportions of

the ellipses could be thought of as angle dependent. The ellipses at constant reference current amplitude are shown in Figure 7-12.

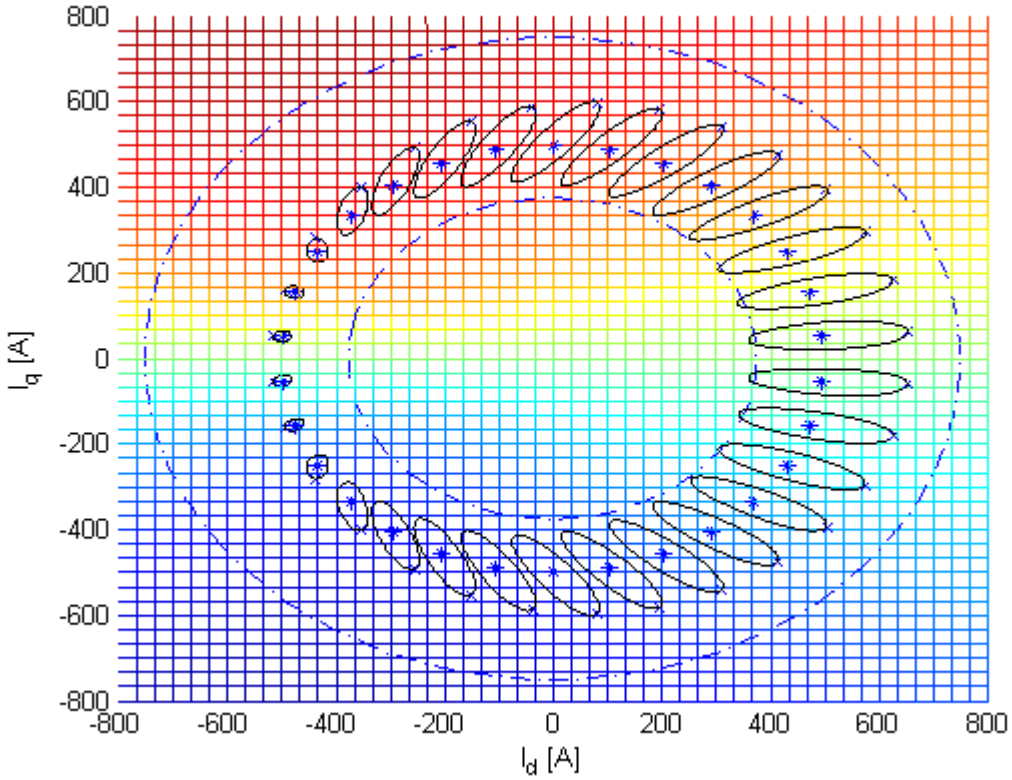

Figure 7-12 Ellipses at constant radius

If the angle is lost it should be possible to detect this and compensate using a table with calculated or measured directions and length/width proportions of the ellipses for all current vector radiuses. The direction and proportion of the ellipses from the high frequency current response is calculated continuously and compared with ellipses in the correction table for that specific current vector length. If a better match is made for an ellipse on an angle deviating from the believed angle a correction is made.

The idea could be represented graphically. By a fault the angle is misaligned over 90 electrical degrees. When a current vector is applied in what is believed to be in positive q axis the high frequency response will look like the red ellipse in Figure 7-13. The direction and proportion of that hf-current response is compared to how the ellipse is supposed to look like should the angle be correct. In Figure 7-14 the best match is found and the angle error is obvious and can be compensated for.

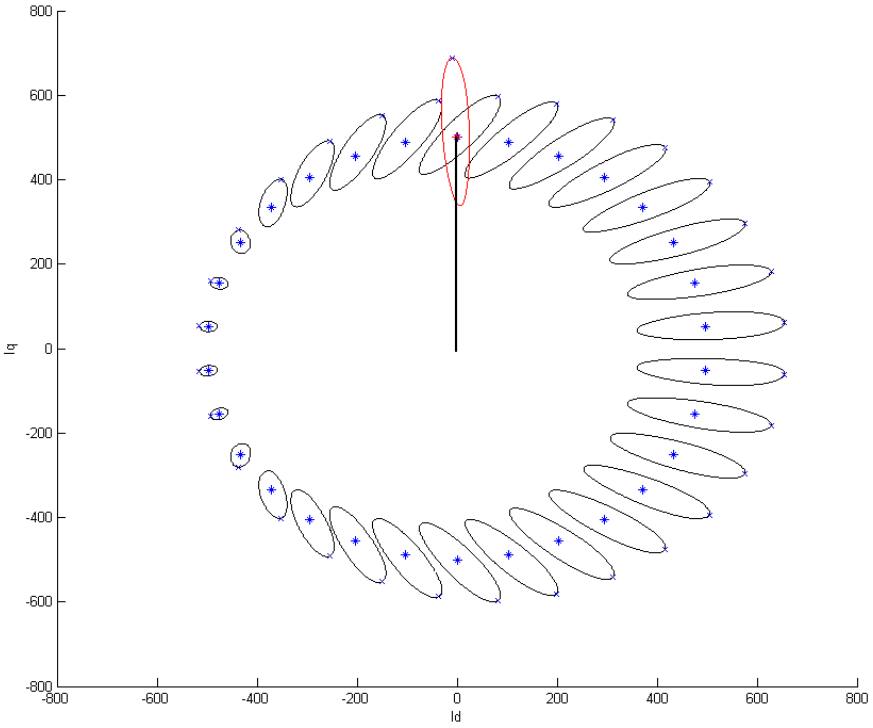

Figure 7-13 Received ellipse without compensation

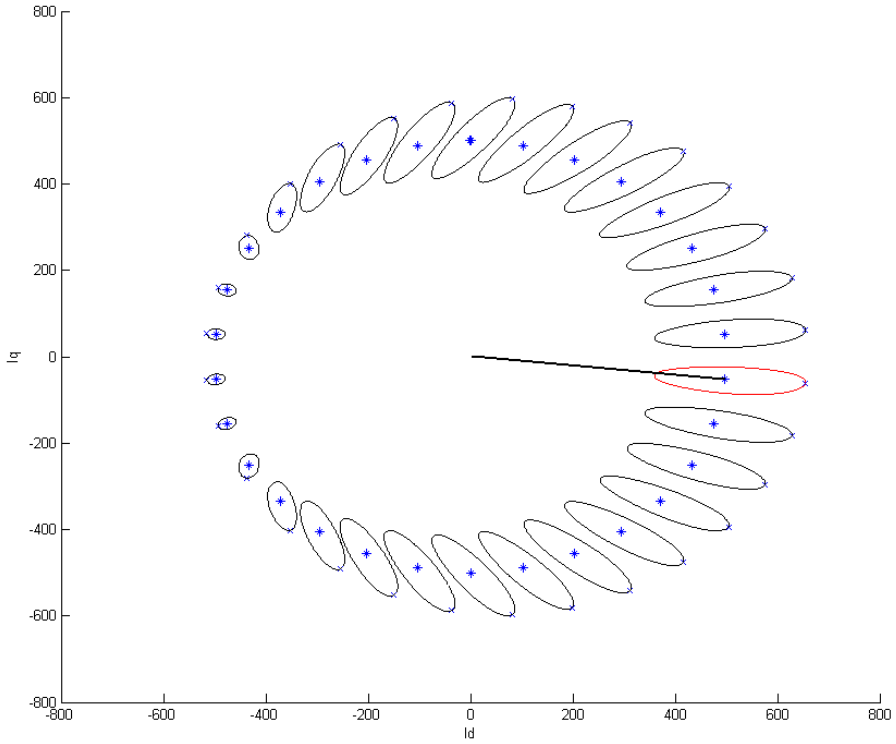

Figure 7-14 Received ellipse with compensation

This method can also be used to assure that the angle don't start to drift away from the correct rotor position angle.

In a real control system it is extremely important to quickly detect and take action on a faulty angle. A high torque reference results in high i_q and if the angle would suffer a large deviation a number of dangerous scenarios are possible. The most obvious is that a large offset would cause torque in the other direction than what was intended. An accident is not an unlikely result from this. Another risk is an angle deviation causing a large negative d-axis flux which could results in complete demagnetization of the permanent magnets, rendering the machine useless.

The compensation method described in this sub section has not been implemented in the Simulink model of the control system due to time constraints. Its performance was accordingly not evaluated.

7.2 Response time of the sensorless system

The simulation results in Chapter 6 showed problems in the position detection when the current was changed rapidly to achieve an alteration in produced torque. This problem is found to originate from the non ideal filters used in the control system filtering out the high frequency current response used for the position detection. A non ideal filter will introduce a delay to the system making the filtered signal distorted for some time after the applied step. In the middle plot in Figure 7-15 it is evident that the distortion causes the pattern where the high peak represents the alignment with the positive d axis to disappear. This makes it impossible to determine the correct position for some time after the step has been applied making the angle error in the lower plot to vary before the constant angle offset caused by cross saturation appears.

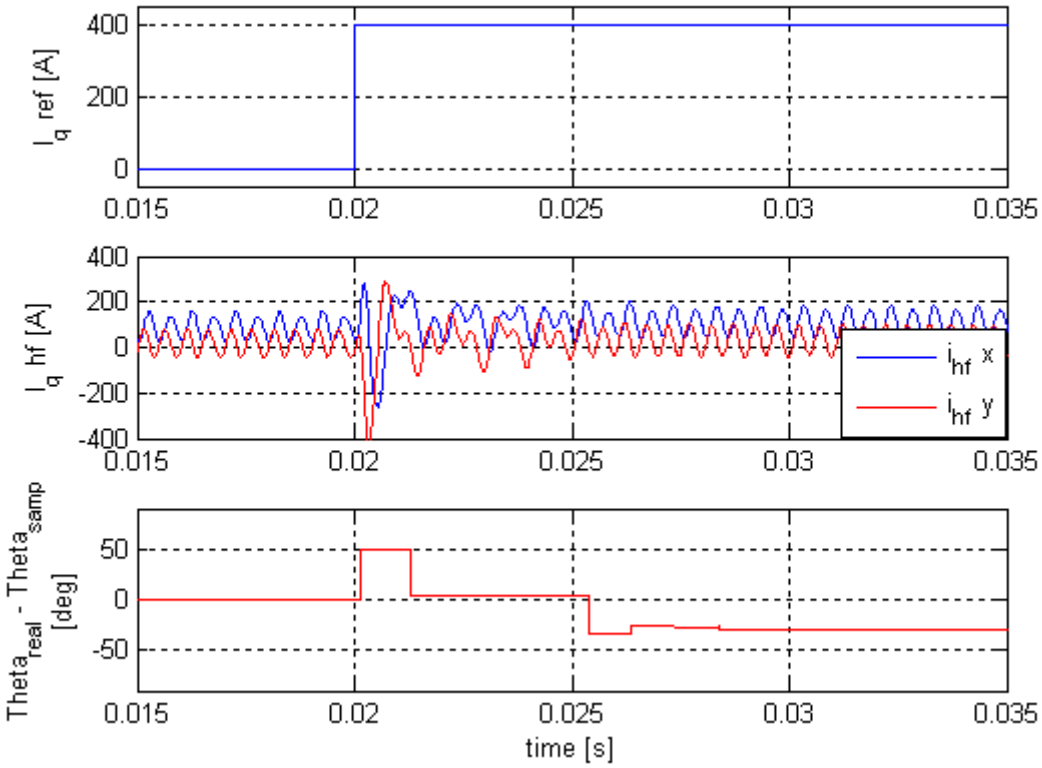

Figure 7-15 Angle error during a reference step

It is desirable to have filters that remove as much as possible of the frequencies that are not used for the position detection. A filter with high order increases the control of which frequencies that are removed and which are allowed to pass, the delay of the filter will however increase with the order of the filter. This means a trade of situation, making the design of the system more complicated. To accomplish a system with good performance, much room for optimizations in the control system and its filters exist.

With an optimized system it would still not be possible to change the reference current in steps as the position still would be lost momentarily, something that not is an acceptable condition. Instead the reference should be increased with for example a ramp function. The increased rise time will allow the filters to keep filtering out the high frequency current response without introducing the noise seen in Figure 7-15. The disturbance in the hf-currents in the middle plot can then be reduced; hence the angle error caused by the step gets smaller making it possible to control the system during changes in the current reference. This is illustrated in Figure 7-16.

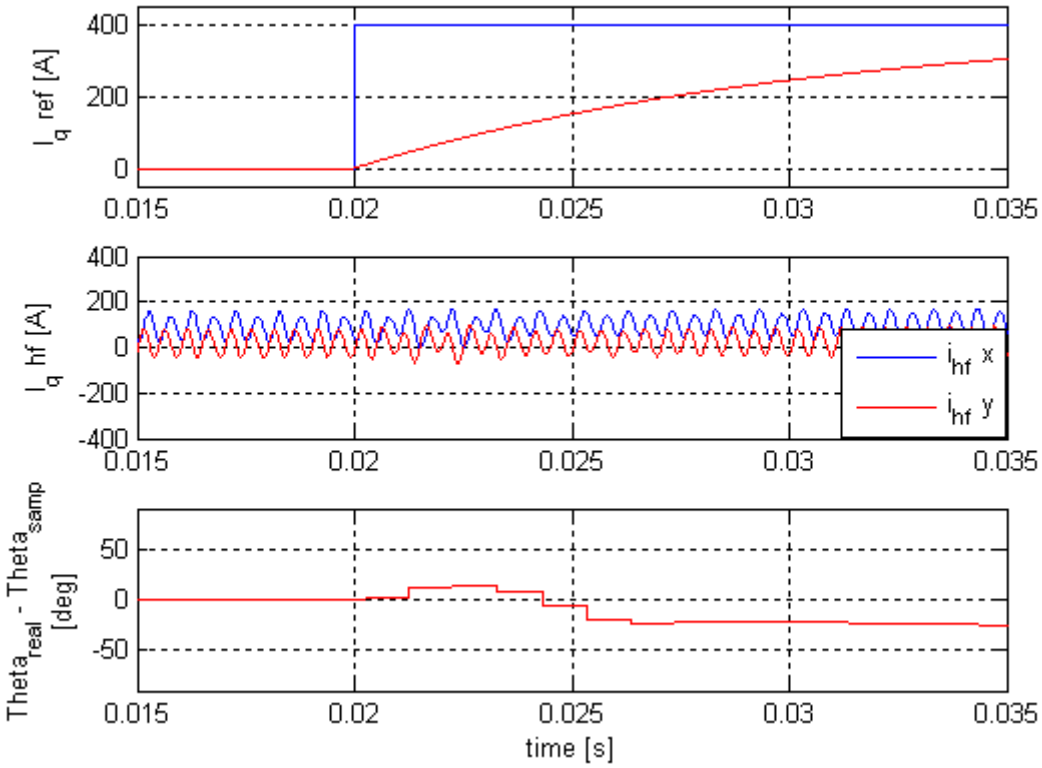

Figure 7-16 Angle error during a slow reference step

Depending of how optimized the system is this ramp can be implemented with different steepness. How much the system can be optimized and how fast response time that can be expected from a system using a sensorless control system has not been evaluated.

7.3 The machine geometries influence on sensorless performance

7.3.1 Prerequisites

In the geometry of the PMSM there are many parameters to change that could affect the behavior of the machine. The phenomena that the signal injection theory is based on is however the saliency of the rotor, described in Chapter 3.2 and 5. Consequently, changes in the rotor configuration are studied. The magnet thickness appeared to be an important parameter as it according to theory should reduce the inductance in the d axis significantly, causing the motor to become more salient.

7.3.2 Different rotor geometries

A large number of geometries with V shaped magnets were created in the simulation environment. The magnet thickness as well as the distance D_1, D_2 and D_3 shown in Figure 7-17 was varied.

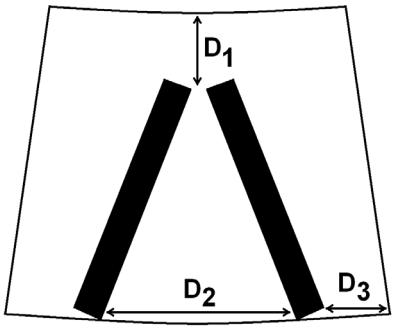

Figure 7-17 Varied distances in the rotor geometry

This rendered a large variety of different geometries and those with the same permanent magnet flux linked to the stator were then selected for further comparison. Some of the more extreme designs are shown in Figure 7-18 to Figure 7-21.

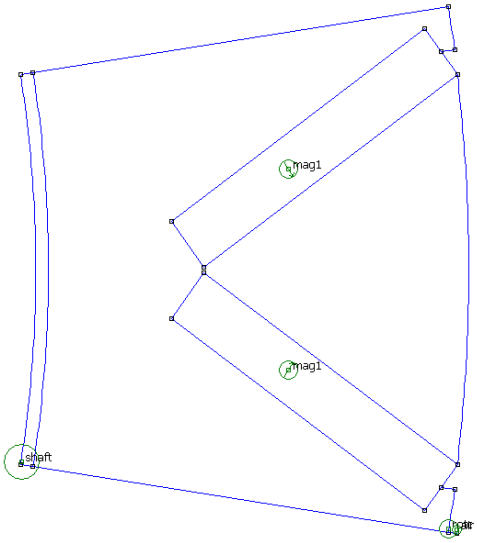

Figure 7-18 FEM model of rotor configuration

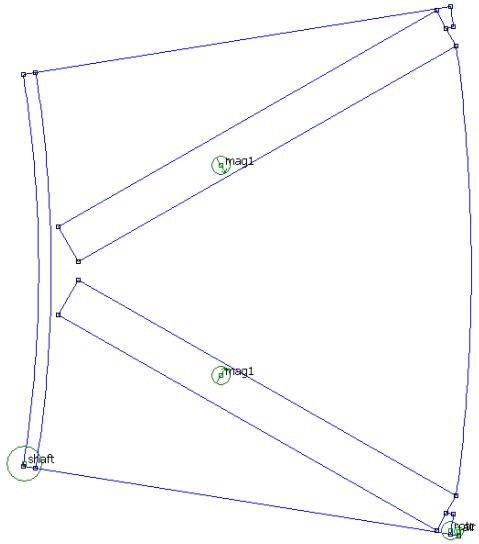

Figure 7-19 FEM model of rotor configuration

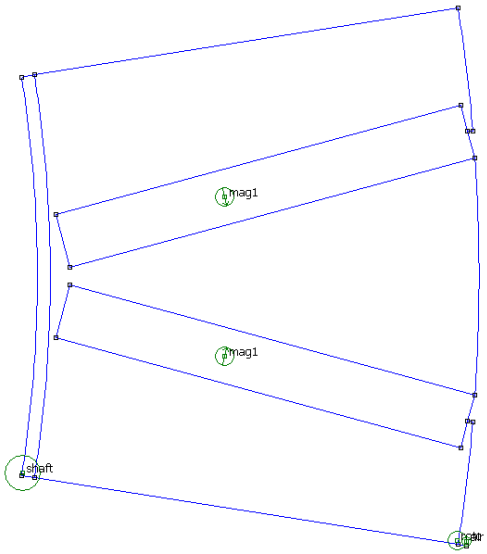

Figure 7-20 FEM model of rotor configuration

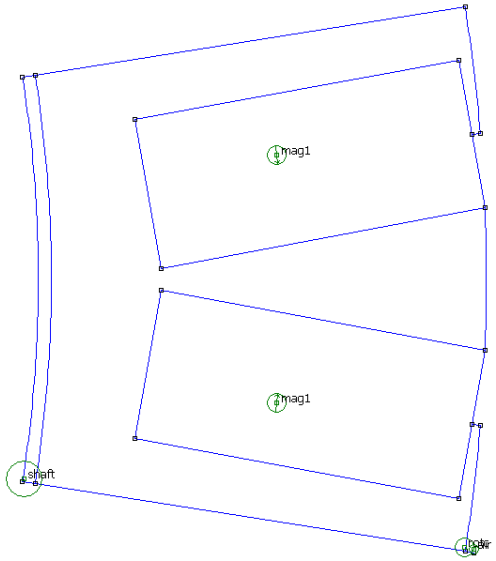

Figure 7-21 FEM model of rotor configuration

7.3.3 Evaluation

The different geometries all showed to have similar characteristics, important differences could however be spotted.

Extremely long and thin magnets like the one in Figure 7-19 have the large drawback that the q-axis flux path gets heavily compromised. When the magnets are made very long the q-axis flux will be more and more forced to take the path through the magnets. This will make the ratio between d- and q-inductance very small as there will be a similar reluctance in the d- and q-axis flux path. The sensorless performance will then be poor as well as the ability to produce reluctance torque. In Figure 7-21 there is a path for the q-axis flux which will make the desirable difference in d- and q-axis inductance larger, this geometry will however show to suffer from some other problems.

The iron between magnet pairs is the place where the path of d- and q-axis flux will meet, consequently it is where the cross saturation will be worst. In Figure 7-19 it can be seen that there are less iron available for the fluxes to meet compared to in Figure 7-20. The iron will then be saturated at lower current levels making the cross saturation more significant. This is seen when studying the d- and q-flux surfaces for the different cases, the contours are sharper. It can also be seen when the rotating high frequency flux vectors from the sensorless system is plotted. The direction of the highest reluctance will deviate more from the d axis due to the increased cross saturation.

If the angle in the V shape of the magnets are decreased too much in an effort to increase the available iron between the magnet pairs another problem can arise. The distance S_2 in Figure 7-22 will be more equal to the distance S_1, making the leakage flux through S_1 much larger. To keep the same permanent flux seen from the stator, the width of the magnets as well as the length has to be increased. That is why the magnets in Figure 7-21 are so much larger compared to the other geometries. By using large magnets it could be imagined that the d-axis inductance would be much smaller than the inductance in q-axis. The leakage flux will however saturate the small q-axis path above the magnets, decreasing the q inductance as well making the inductance ratio smaller.

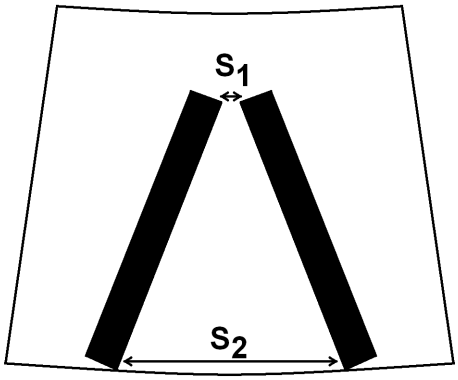

Figure 7-22 Illustration of the spaces between the magnets in one magnet pair

7.3.4 Favourable properties of the rotor geometry

By the results from subsection 7.3.3 it is possible to summarize some of the properties for a rotor design with good sensorless performance.

To minimize problems with regular saturation it is important that the path for the q axis flux is not easily saturated. This is accomplished by keeping the smallest width of the path large enough. The areas where problems are likely to occur are marked with dots in Figure 7-23.

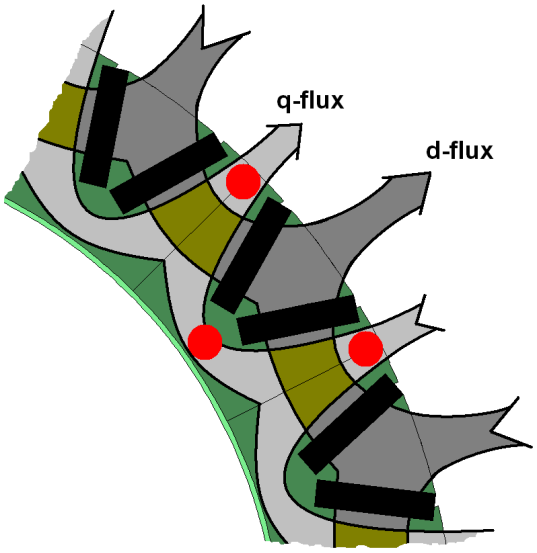

Figure 7-23 Problem areas regarding the q-axis path saturation

In order to reduce cross saturation effects it is positive to keep the distance between the V magnet pairs large. This is the area where the d- and q-axis flux paths meet and it is advantageous to have much iron there to reduce the saturation. The problem areas are illustrated in Figure 7-24.

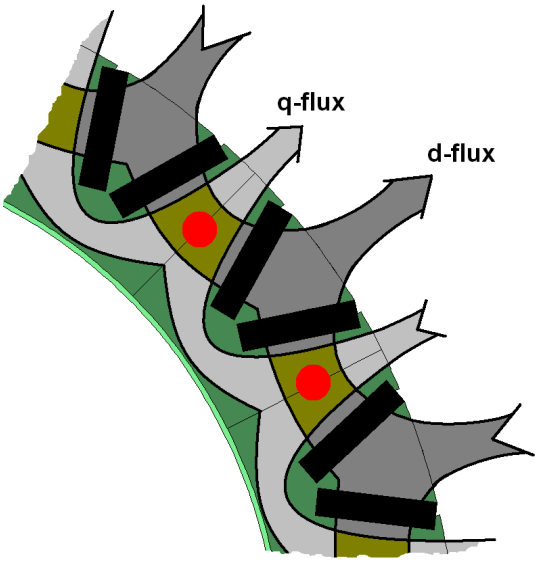

Figure 7-24 Problem areas regarding cross saturation

It is also important not to decrease the angle in the V shape of the magnet too much, this as the leakage flux increases with the angle reduction. Too much leakage flux could cause serious problems to the q-axis flux path as flux with no useful purpose is added.

To get a large ratio between d-and q-axis inductance it is important that the q-axis flux path is not easily saturated, but also that the permanent magnets are thick as this is what to a large extent determines the d-axis inductance. Making the magnets very thick gives a large reduction in d-axis inductance; the disadvantage with this is that higher current is needed for field weakening.

8 Conclusions

To accomplish a sensorless control system of a PMSM the back-EMF method has to be combined with a signal injection method for low and zero speed. At medium and high rotational speeds the back-EMF method is well tested and is a reliable choice, but since the back EMF vector is speed dependent, hence diminishes at low speed, a transition to signal injection must be done. Considering that the signal injection method is not yet fully developed, the focus in this paper has been put on understanding the problems and trying to suggest improvements that can facilitate the rotor detection for low and zero speed (up to 5 electrical Hz).

Signal injection requires a magnetical asymmetry in the rotor leading to a difference between the d- and q-inductances (the d-axis direction in the rotor will have the lowest inductance). This asymmetry can originate from the physical design of the rotor, essentially from the placement of the permanent magnets. It can also be caused by saturation and cross saturation effects in the machine. In a normal modern rotor these saturation effects are evident.

Using signal injection means adding a voltage vector with constant length, rotating with a high frequency in the αβ-system. This creates a rotating flux vector with constant amplitude in the motor. Due to the constant amplitude of the flux vector, the current response will fluctuate depending on how the inductance in the rotor is varying. The knowledge of the direction of the rotating flux vector at every instant in combination with measuring the length of the responding current vectors, gives the d-axis direction as equal to the direction of the injected flux at the instant when the current vector reaches a maximum. The signal injection method is explained and illustrated in detail in the thesis.

It is concluded that when large torque producing currents are applied to the motor, the cross saturation in the rotor will be more and more evident, causing the direction of the lowest dynamic inductance to be displaced from the d-axis direction. This means that the direction of the maximum current vector no longer will equal the d-axis direction; hence there will be an offset between the detected and the real rotor angle. This will cause problems with all methods that uses signal injection. The deviation is however depending on the applied current and it has been shown that by characterizing its effect by measurements it can to a large extent be compensated for with for example a lookup table.

It is further shown that saturation effects also can be made useful. In the developed signal injection method the saturation in the d-axis flux is used to determine the polarity of the rotor. If the iron materials had been linear, the polarity would have been impossible to establish since the rotor is structurally symmetrical in positive and negative d-direction.

Rapid current changes are identified as a problem in the sensorless control system. The filters used to filter the useful high frequency current are not ideal and will require some time to adapt when the amplitude of the torque producing current is changed. To keep the angle error low during a change of applied current, the rise time of the current had to be limited. By optimizing the control system and the filters the performance could probably be improved, but whether the sensorless system can be made as fast as a system with a mechanical position sensor is still to be resolved.

Extensive changes in the machine configuration were made, primarily regarding the magnet design and placement in the rotor, showing that the performance of the sensorless control can be increased. This was proven possible without compromising the torque production capabilities in the rotor. To avoid problems with a small ratio between the d- and q-axis inductances (L_d and L_q), the path for the q-axis flux should not be easily saturated. In order to reduce cross saturation effects it was found positive to keep the distance between the V

shaped magnet pairs large. This is the area where the d- and q-axis flux paths meet and it is advantageous to have much iron there to reduce the saturation. It is also important not to decrease the angle in the V shape too much as this means much permanent magnet leakage flux, that will saturate the q-axis flux path. The consequence is that the q-inductance decreases, hence the ratio between L_d and L_q will be smaller, in combination with a demand for more magnet material as the magnets would have to be larger to produce equally much flux linking with the stator windings.

A large inductance ratio can be achieved by decreasing the d-axis inductance. This will however be disadvantageous if the machine is used in field weakening as this is obtained by creating a flux in negative d direction, counteracting the permanent magnet flux. If the d-axis inductance is small, the current needed to produce the necessary amount of negative d-axis flux will have to be high, resulting in a reduction in the torque producing capabilities in the field weakening region.

Finally, it is concluded that when choosing a machine to use with a sensorless control system a thorough investigation of the machines electromagnetical properties has to be done, as was done in this thesis. Only considering the changes in d- and q-axis inductance is not enough as it does not describe the machines sensorless behavior in a comprehensive manner.

9 Future work

In the model of the PMSM used in the thesis work some simplifications were made. To get better results from the simulations that more equals reality these effects should be added. In the FEM calculations a 2D model of the machine were used, replacing it by a 3D model would add the possibility to incorporate the end windings effect. Even more important could be to add the eddy current effects, this because of the rotating high frequency flux from the signal injection method.

A problem with the sensorless control system showed to be restrictions in the response time caused by delays in the non ideal filters (used to filter out the high frequency response). Improvements in the response time could be done by optimizing the control system and its filters.

To decrease the influence of the cross saturation effects the more advanced compensation method described in Subchapter 7.1.3.2 should be implemented. This would also increase the reliability of the system as it will be able to detect angle deviations caused by failure in the system.

More features could be added to the simulations to make the system more complete. A system working for all speeds could be accomplished by complementing the signal injection with a back-EMF method that is used for higher speeds.

One of the most demanding working conditions for the PMSM in a hybrid powertrain is the cranking of the ICE. By adding a model for this the functionality of the sensorless control system during a more difficult condition could be verified.

The next step of testing the system would be to use a model of the machine attained from measurements on a real machine and ultimately test the system on a real PMSM machine.

10 References

[1] Harnefors L: “Control of Variable-Speed Drives”,
Västerås: Mälardalen University, 2002, pp 62, 93, 167-168

[2] Hughes A: “Electric Motors and Drives”, Third edition
Elsevier Ltd, 2006, ISBN-10: 0-7506-4718-3, pp 353

[3] Skvarenina T L: “The Power Electronics Handbook”,
CRC Press LCC, 2002, ISBN: 0849373360

[4] Rashed M, MacConnell P F A, Stronach A F, Acarnley P: ”Sensorless Indirect-Rotor-Field-Orientation Speed Control of a Permanent-Magnet Synchronous Motor With Stator-Resistance Estimation”, *IEEE Transactions On Industry Electronics,Vol. 54, No. 3*, June 2007, pp 1664-1675

[5] Advanced Micro Controls Inc: “What is a resolver?”,
http://www.amci.com/tutorials/tutorials-what-is-resolver.asp, (Accessed: 2008-01-04)

[6] Webster J G: "Measurement Instrumentation and Sensors Handbook The",
CRC Press LCC, 1999, ISBN: 084932145X

[7] Bishop R H: "Mechatronics Handbook The",
CRC Press LCC, 2002, ISBN: 0849300665

[8] Bocker J, Kroger C: ”Control of permanent magnet synchronous motor with dual-mode position estimation”, EPE Dresden, 2005, ISBN: 90-75815-08-5

[9] Morimoto S, Sanada M, Takeda J: ”3-phase High Frequency Voltage Input Sensorless Control for Hybrid Electric Vehicle Applications” *The 22nd International Battery, Hybrid and Fuel Cell Electric Vehicle Symposium & Exposition*, Oct. 23-28, 2006, pp 458-467

[10] Arias A, Saltiveri D, Caruana C, Pou J, Gago J, Gonzalez D: ”Position estimation with voltage pulse test signals for Permanent Magnet Synchronous Machines using Matrix Converters”, *5th International Workshop – CPE,* 2007

[11] Miranda R S, Jacobina C B, Femandes E M, Lima A M N, Oliveira A C, Correa M B R: ”Parameter and Speed Estimation for Implementing Low Speed Sensorless PMSM Drive System Based on an Algebraic Method”, *Applied Power Electronics Conference, APEC 2007 - Twenty Second Annual IEEE*, Feb. 25 2007 - March 1 2007, pp 1406-1410

[12] Corley M J, Lorenz R D: ”Rotor Position and Velocity Estimation for a Salient-Pole Permanent Magnet Synchronous Machine at Standstill and High Speeds”, *IEEE Transactions On Industry Applications, Vol. 34, No. 4*, July/August 1998, pp 784-789

[13] Wallmark O, Harnefors L, Carlson O: ”Sensorless Control of PMSM Drives for Hybrid Electric Vehicles”, *35th Annual IEEE Power Electronics Specialists Conference. Aachen, Germany*, 2004

[14] Persson J, Markovic M, Perriard Y: ”A New Standstill Position Detection Technique for Nonsalient Permanent-Magnet Synchronous Motors Using the Magnetic Anisotropy Method”, *IEEE Transactions On Magnetics, Vol. 43, No. 2*, February 2007, pp 554-560

[15] Tursini M, Petrella R, Parasiliti F: ”Sensorless control of an IPM synchronous motor for city-scooter applications”, *Industry Applications Conference, 2003. 38th IAS Annual Meeting. Conference Record of the, Volume 3*, 12-16 Oct. 2003, pp 1472-1479

[16] Kim H, Lorenz R.D: ”Carrier signal injection based sensorless control methods for IPM synchronous machine drives”, *Industry Applications Conference, 2004. 39th IAS Annual Meeting. Conference Record of the 2004 IEEE, Volume* 2, 3-7 Oct. 2004, pp 977-984

[17] Arias A, Saltiveri D, Caruana C, Pou J, Gago J, Gonzalez D: ”Position estimation with voltage pulse test signals for Permanent Magnet Synchronous Machines using Matrix Converters”, *Compatibility in Power Electronics, 2007. CPE '07,* May 29 - June 1 2007, pp 1-6

[18] Yan Y, Zhu J, Guo Y, Lu H: ”Modeling and Simulation of Direct Torque Controlled PMSM Drive System Incorporating Structural and Saturation Saliencies”, *Industry Applications Conference, 2006. 41st IAS Annual Meeting. Conference Record of the 2006 IEEE, Volume 1*, Oct. 2006, pp 76-83

[19] Norling C, Österman J: “Physics Handbook for Science and Engineering”, Sixth edition, ISBN: 9144008236, Lund: Studentlitteratur, 2002, pp 48

[20] Linke M, Kennel R, Holtz J: ”Sensorless speed and position control of permanent magnet synchronous machines using alternating carrier injection”, University of Wuppertal, 2003

[21] Zhuang X, Rahman M F: ”An Adaptive Sliding Stator Flux Observer for a Direct-Torque-Controlled IPM synchronous Motor Drive”, *IEEE Transactions On Industry Electronics, Vol. 54, No. 5*, October 2007, pp 2308-2406

[22] Qiujian G, Li Z, Feng Z, Xuhui W: ”A Novel Sensorless Control Method for IPM Synchronous Machine Drives by Carrier Signal Injection based on Magnetic Saliency”, *IEEE Industrial Electronics, IECON 2006 - 32nd Annual Conference on*, Nov. 2006, pp 1023–1028

[23] Nondahl T A, Ray G, Schmidt P B: ”A permanent magnet rotor containing an electrical winding to improve detection of motor angular position”, *Industry Applications Conference, 1998. Thirty-Third IAS Annual Meeting. The 1998 IEEE, Volume 1*, 12-15 Oct. 1998, pp 359-363

[24] Consoli A, Scarcella G, Testa A: “Industry application of zero-speed sensorless control techniques for PM synchronous motors”, *Industry Applications, IEEE Transactions on, Volume 37, Issue 2,* March-April 2001, pp 513-521

[25] Choi C, Seok J: “Compensation of Zero-Current Clamping Effects for Sensorless Drives Based on High-Frequency Signal Injection”, *Industry Applications Conference, 2006. 41st IAS Annual Meeting. Conference Record of the 2006 IEEE, Volume 5,* 8-12 Oct. 2006, pp 2466-2471

[26] Guerrero J M, Leetmaa M, Briz F, Zamarron A, Lorenz R D: ”Inverter nonlinearity effects in high-frequency signal-injection-based sensorless control methods”, *Industry Applications, IEEE Transactions on, Volume 41, Issue 2*, March-April 2005, pp 618-626

[27] Hu J, Xu L, Liu J: ”Eddy Current Effects on Rotor Position Estimation for Sensorless Control of PM Synchronous Machine”, *Industry Applications Conference, 2006. 41st IAS Annual Meeting. Conference Record of the 2006 IEEE, Volume 4*, 8-12 Oct. 2006, pp 2034-2039

[28] Silva C, Asher G M, Sumner M: ”Hybrid rotor position observer for wide speed-range sensorless PM motor drives including zero speed”, *IEEE Transactions On Industry Electronics, Vol. 53, No. 2*, April 2006, pp 373-378

[29] Itoh J, Nomura N, Ohsawa H: ”A comparison between V-f control and position-sensorless vector control for the permanent magnet synchronous motor”, *Power Conversion Conference, Osaka 2002, Volume 3*, 2-5 April 2002, pp 1310-1315

[30] Piippo A, Salomaki J, Luomi J: ”Signal Injection in Sensorless PMSM Drives Equipped With Inverter Output Filter”, *Power Conversion Conference - Nagoya, 2007*. 2-5 April 2007, pp 1105-1110

[31] Rieder U H, Schroedl M: ”A simulation method for analyzing saliencies with respect to enhanced INFORM-capability for sensorless control of PM motors in the low speed range including standstill”, *Power Electronics and Applications, 2005 European Conference on, 11-14 Sept.*, 2005, pp 8

[32] Avo Reinap, Doctor at Industrial Electrical Engineering and Automation, Lund University, Sweden

[33] Arata M, Takahashi N, Sakai K, Hagiwara K, Araki T: ”Large Torque and High Efficiency Permanent Magnet Reluctance Motor for A Hybrid Truck”, *The 22nd International Battery, Hybrid and Fuel Cell Electric Vehicle Symposium & Exposition,* Oct. 23-28 2006, pp 534-539

[34] Shigeo M, Hideya A, Masayuki S, Yoji T: “Interior Permanent Magnet Synchronous Motors Mainly Using Reluctance Torque”, *Transactions of the Institute of Electrical Engineers of Japan, Vol.119, No.10*, 1999, pp 1177-1183

Appendix A Flux linkage to current transformation

The Matlab code shown below is performing the transformation from flux as a function of d- and q axis currents to current as a function of d- and q axis flux. The goal is to find at what currents a certain combination of d and q axis flux is created. To achieve this, the contour lines for the wanted fluxes are calculated in the flux surfaces. This gives the combinations of I_d and I_q that could create the d axis flux and which combinations that could create the q axis flux. By calculating the crossing point between the two contour lines the one combination of I_d and I_q that creates that specific d and q axis flux is found.

The extract is a part of the code written to the thesis.

```
%Calculates the currents Id and Iq as a function of the linked fluxes Psid and Psiq
  incq=0;
  for Psiq_find=-0.31:0.001:0.31;
     incq=incq+1;
     incd=0;
     Psiq_x(incq)=Psiq_find;
     for Psid_find=-0.2:0.001:0.37;
        incd=incd+1;
        Psid_y(incd)=Psid_find;

        %Calculate the two conturlines as 4 vectors
        Line1=contourc(Psid,[Psid_find Psid_find]);
        y1=Line1(1,2:length(Line1));
        x1=Line1(2,2:length(Line1));
        Line2=contourc(Psiq,[Psiq_find Psiq_find]);
        y2=Line2(1,2:length(Line2));
        x2=Line2(2,2:length(Line2));

        if (length(x1)>0) && (length(x2)>0)
           %The crossing between the two contour lines in the plane is found using polyxpoly
           [xi,yi] = polyxpoly(x1,y1,x2,y2);
           if (length(xi)>0)
              %Interpolate the current at the crossing
              Id_i = interp1(Id,yi);
              Iq_i = interp1(Iq,xi);
              Iq_result(incd,incq)=Iq_i(1);
              Id_result(incd,incq)=Id_i(1);
           else
              Iq_result(incd,incq)=NaN;
```

```
            Id_result(incd,incq)=NaN;
        end
    else
        Iq_result(incd,incq)=NaN;
        Id_result(incd,incq)=NaN;
    end
end
```

Appendix B Model flow chart

The subsystems in the flow chart in Figure 5-8 is shown in Figure B-1 to Figure B-4 below. The current regulator, αβ to three phase transformation, pulse width modulation and low pass filters in Figure 5-8 are not included since no changes has been made to these systems during the thesis work.

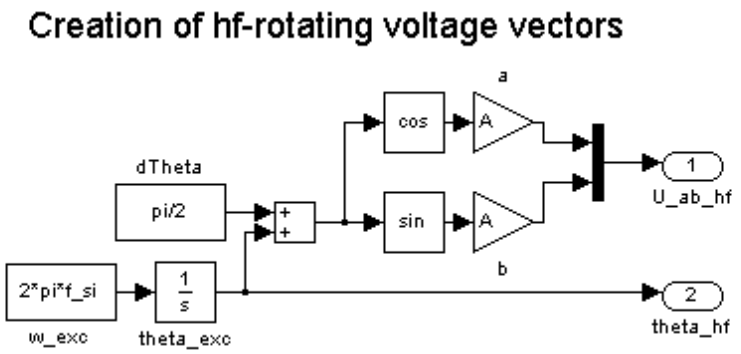

Figure B-1 Signal injection

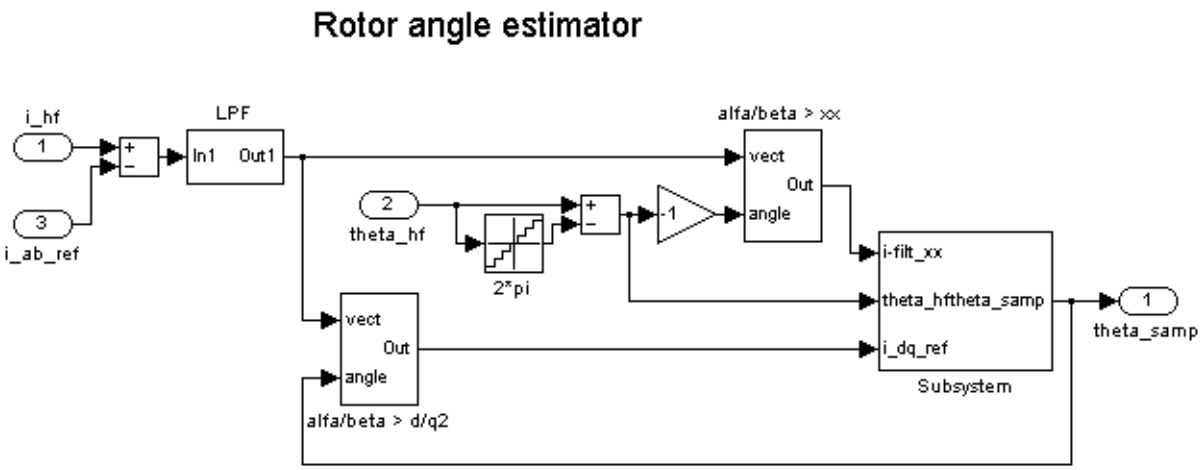

Figure B-2 Rotor angle estimator

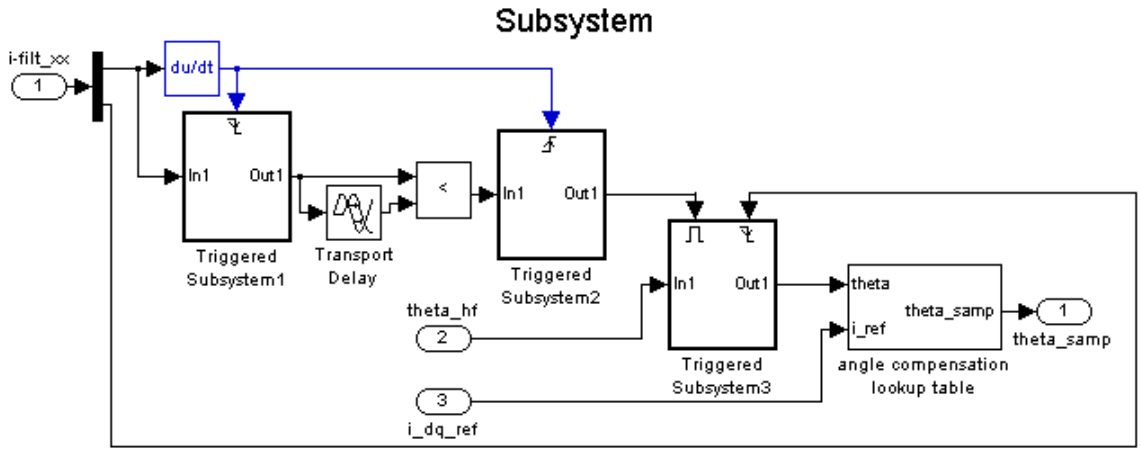

Figure B-3 Subsystem in the rotor angle estimator

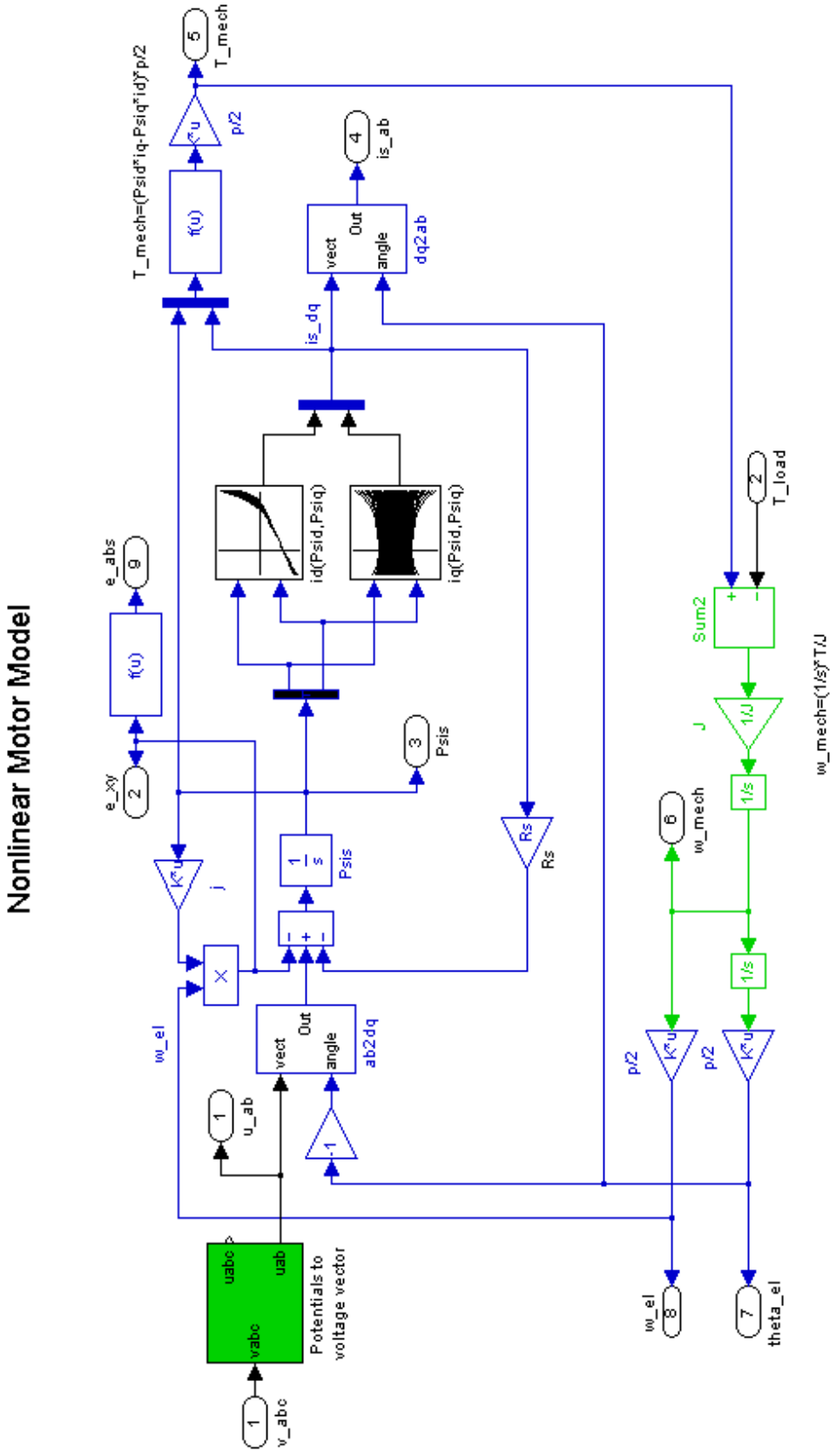

Figure B-4 Nonlinear motor model of the PMSM